JOC The Journal of Organic Chemistry

Article

pubs.acs.org/joc

Regio- and Stereoselective Synthesis of Spiropyrrolizidines and Piperazines through Azomethine Ylide Cycloaddition Reaction

Saoussen Haddad,[†,‡] Sarra Boudriga,[†] François Porzio,[‡] Armand Soldera,[‡] Moheddine Askri,*[,†] Michael Knorr,[§] Yoann Rousselin,[∥] Marek M. Kubicki,[∥] Christopher Golz,[⊥] and Carsten Strohmann[⊥]

[†]Laboratoire de Chimie Hétérocyclique, Produits Naturels et Réactivité/ LCHPNR, Département de Chimie, Faculté des Sciences de Monastir, 5000 Monastir, Tunisie

[‡]Département de Chimie, Centre Québécois sur les Matériaux Fonctionnels, Université de Sherbrooke, Sherbrooke, Québec J1K 2R1, Canada

[§]Institut UTINAM - UMR CNRS 6213, Université de Franche-Comté, 16 Route de Gray, F-25030 Besançon, France

[∥]Institut de Chimie Moléculaire - UMR CNRS 6302, Université de Bourgogne, 9 Avenue A. Savary, F-21078 Dijon, France

[⊥]Anorganische Chemie, Technische Universität Dortmund, Otto-Hahn-Strasse 6, 44221 Dortmund, Germany

Supporting Information

ABSTRACT: A series of original spiropyrrolizidine derivatives has been prepared by a one-pot three-component [3 + 2] cycloaddition reaction of (*E*)-3-arylidene-1-phenyl-pyrrolidine-2,5-diones, L-proline, and the cyclic ketones 1*H*-indole-2,3-dione (isatin), indenoquinoxaline-11-one and acenaphthenequinone. We disclose an unprecedented isomerization of some spiroadducts leading to a new family of spirooxindolepyrrolizidines. Furthermore, these cycloadducts underwent retro-1,3-dipolar cycloaddition yielding unexpected regioisomers. Upon treatment of the dipolarophiles with *in situ* generated azomethine ylides from L-proline or acenaphthenequinone, formation of spiroadducts and unusual polycyclic fused piperazines through a stepwise [3 + 3] cycloaddition pathway is observed. The stereochemistry of these N-heterocycles has been confirmed by several X-ray diffraction studies. Some of these compounds exhibit extensive hydrogen bonding in the crystalline state. To enlighten the observed regio- and stereoselectivity of the [3 + 2] cycloaddition, calculations using the DFT approach at the B3LYP/6-31G(d,p) level were carried out. It was found that this reaction is under kinetic control.

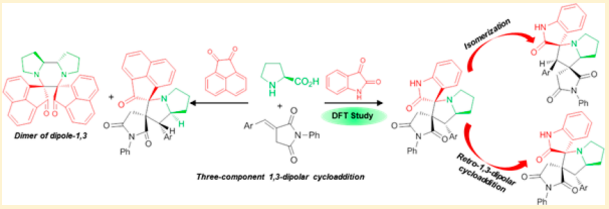

INTRODUCTION

Synthesis of derivatives of natural products is particularly attractive, especially if it ultimately leads to biological activities. In this context, the potential of pyrrolizidine derivatives was not exploited sufficiently. The latter have attracted a great deal of interest because of their frequent occurrence in natural products and their significant biological activities.[1,2] In particular, multifunctional polycyclic spiropyrrolizidines contain a privileged heterocyclic skeleton that is found in a large family of synthetic compounds exhibiting versatile bioactivities, such as antimycobacterial,[3] antitumor,[4] antimicrobial,[5] antibacterial,[6] antifungal,[7] and antiviral[8] properties. The spiropyrrolizidine unit also occurs in several natural products, such as peteropodine, isopeteropodine, mitraphylline,[9] and spirotryprostatin A[10] (Figure 1). Efficient synthesis of such molecules is thus of particular relevance, therefore we propose in this report a new one-pot synthesis of spiropyrrolizidines derivatives.

Driven by thorough investigation of the biological activities of this class of compounds, much attention has been focused on the development of efficient methodologies for the preparation of structurally diverse spiropyrrolizidines. The actual multicomponent 1,3-dipolar cycloaddition of electron-deficient alkenes with azomethine ylides generated *in situ* via decarboxylative condensation of cyclic ketones and L-proline provides a very effective tool to access spiropyrrolizidine containing compounds.[11] Its process simplicity, mild reaction conditions, atomic economy, and extension of the scope of substrates made it a current route in combinatorial chemistry. On the other hand, the pyrrolidine-2,5-dione scaffold is a central component of numerous alkaloids as well as a great variety of synthetic compounds endowed with diverse bioactivities, including anticonvulsant,[12] antimycobacterial,[13] and antidepressant properties.[14] Recently, we have reported the synthesis of new functionalized spirooxindolepyrrolidines and dispiropyrrolothiazoles incorporating the pyrrolidine-2,5-dione motif. Some representative molecules exhibiting antibacterial, antifungal, antimalarial, and antimycobacterial activities are shown in Figure 2.[15] Prompted by the synthetic interest and applications of spiropyrrolizidine and pyrrolidine-2,5-dione skeletons as part of our research on N-spiroheterocycles,[16] we describe herein the synthesis of a novel series of spiropyrrolizidines via one-pot multicomponent 1,3-dipolar cycloaddition reaction of (*E*)-3-arylidene-1-phenyl-pyrrolidine-2,5-diones

Received: June 19, 2015
Published: August 20, 2015

ACS Publications © 2015 American Chemical Society

DOI: 10.1021/acs.joc.5b01399
J. Org. Chem. 2015, 80, 9064−9075

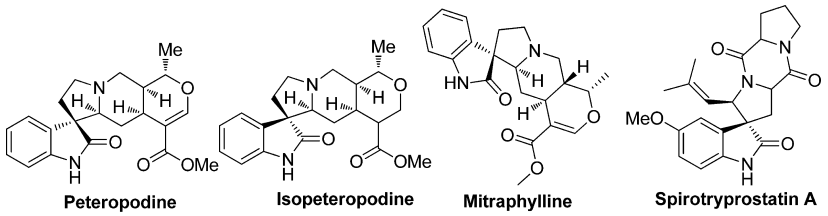

Figure 1. Examples of naturally occurring spiropyrrolizidine-derived alkaloids.

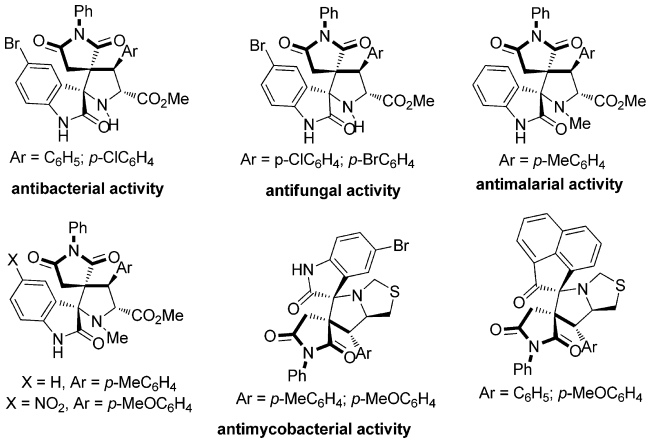

Figure 2. Representative examples of bioactive synthesized compounds incorporating a pyrrolidine-2,5-dione motif.

with azomethine ylides.[17] The latter have been generated *in situ* by reaction of various cyclic ketones and L-proline.

Cycloaddition reaction of exocyclic α,β-unsaturated ketones with azomethine ylide derived from L-proline and isatin exclusively leads to dispiropyrrolizidine with two adjacent spiro-carbons, while formation of the other regio- and stereoisomers has never been reported (Scheme 1).[11] We

Scheme 1. Profile of the 1,3-Dipolar Cycloaddition of Exocyclic α,β-Unsaturated Ketones across Azomethine Ylides Derived from L-proline and Isatin[a]

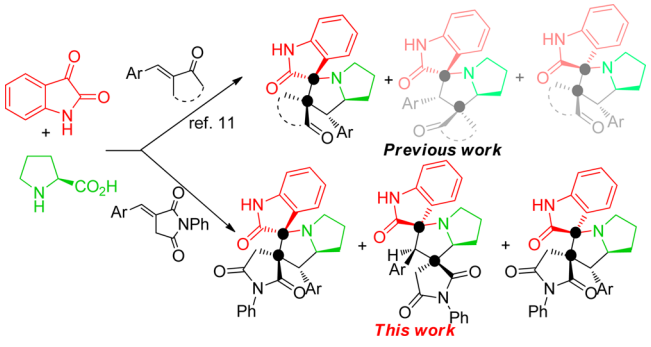

[a]The "•" denotes a spiranic carbon.

thus describe for the first time the formation of the hitherto unknown regioisomer. Moreover, we revealed an unprecedented epimerization of some spirooxindolepyrrolizidines (Scheme 1). To our knowledge, such regio- and diastereodivergent cycloadditions have not been reported yet. To support our findings, we carried out calculations at the quantum level. Theoretical investigations on the reaction of acyclic alkenes with azomethine ylides derived from L-proline and isatin have been reported recently.[18] However, there are no reports on the cycloaddition of exocyclic alkenes with this type of 1,3-dipole. Density functional theory (DFT) was thus used to rationalize the unusual regio- and diastereoselectivity of this kind of reaction.

RESULTS AND DISCUSSION

Three-Component Synthesis of the Spiropyrrolizidines 4–6. To optimize the reaction conditions, the three-component reaction of isatin **1a**, L-proline **2** and (*E*)-3-arylidene-1-phenylpyrrolidine-2,5-dione **3d** (Ar = *p*-ClC_6H_4) was chosen as a model (Table 1). In order to evaluate both the effect of solvent and temperature, the reaction was conducted at different temperatures in acetonitrile and methanol as reaction media. The collected data presented in entries 1–6 of Table 1 indicate that the regio- and stereoselectivity of this reaction are both solvent- and temperature-dependent. This optimization study revealed that the best results were obtained by refluxing the reaction mixture in methanol for 0.5 h, providing spirooxindolepyrrolizidine **4d** with an excellent yield (85%) (Table 1, entry 4). However, a prolongation of the reflux time (24 h) afforded an isomeric mixture of **4d**:**5d**:**6d** in a 57:24:19 ratio (Table 1, entry 5). This finding is in contrast to the commonly observed regio- and stereoselectivity outcome in these type of 1,3-dipolar cycloaddition reactions.[11,17]

Having established suitable reaction conditions (Table 1, entry 5), we tried to extend the scope of this reaction using a series of different *p*-aryl substituted dipolarophiles **3**. This was done with the objective to examine the influence of the electronic effects exerted by the substituent at the *p*-position of the aryl group of imides **3** on the outcome of the reaction (Table 2). As shown in Table 2, reaction of imides **3a–e** yielded the two regioisomers **4** and **5** along with the diastereoisomers **6** (Table 2, entries 1–5). Independently of the M-effect of the *p*-aryl substituent, isomer **4** is the dominant one in all entries. The reaction mixture has been separated by column chromatography.

Spectroscopic and Crystallographic Characterization of the Isomeric Cycloadducts. The structure and the relative configuration of the isomeric spiropyrrolizidines resulting from the cycloaddition were deduced in solution from their NMR data and in the solid state from three X-ray structure determinations performed on cycloadducts **4e**, **5d**, and **6d**. Selected chemical shift values and NOE correlation of spiropyrrolizidines **4d**, **5d**, and **6d** are indicated in Figure 3. The ^{1}H NMR spectra of **4d** and **6d** show two mutually coupled doublets centered at 2.68 and 3.31 ppm (J = 18.7 Hz for **4d** and 18.1 Hz for **6d**) corresponding to the diastereotopic 4′-CH_2 group. Furthermore, the protons H-4 usually appears as a doublet at δ 4.05 and 5.05 ppm in **4d** and **6d**, respectively. Their coupling constants of approximately 9 Hz indicate that this proton is *trans*-arranged with respect to vicinal proton H-4a. This proton gives rise to a multiplet at 4.62–4.69 ppm and at 4.20–4.28, in **4d** and **6d**, respectively. The occurrence and

DOI: 10.1021/acs.joc.5b01399
J. Org. Chem. 2015, 80, 9064–9075

Table 1. Reaction Conditions Employed for the Synthesis of Spiroyrrolizidines 4d, 5d, and 6d[a]

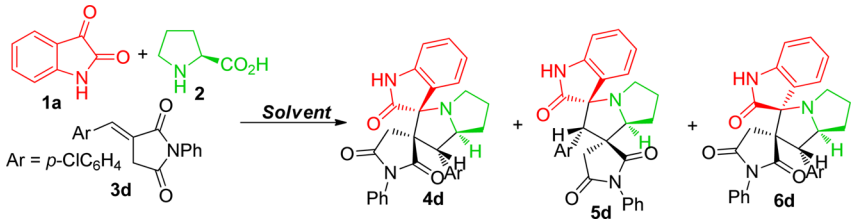

entry	solvent	T (°C)	time (h)	yield (%)[b]	ratio[c] **4d:5d:6d**
1	CH_3CN	80	2	70	100:00:00
2	CH_3CN	80	36	70	72:18:10
3	CH_3CN	24	5	65	100:00:00
4	MeOH	64	0.5	85	100:00:00
5	**MeOH**	**64**	**24**	**85**	**57:24:19**
6	MeOH	25	24	NR[d]	–

[a]The reactions were carried out with **1a** (0.5 mmol), **2** (0.75 mmol), and **3d** (0.5 mmol) in solvent (10 mL). [b]Overall yields after isolation of the products by column chromatography. [c]Relative ratios were determined by ^{1}H NMR from the crude reaction mixture. [d]No reaction due to insufficient solubility.

Table 2. Synthesis of Spiropyrrolizidines 4−6 via Three-Component Reaction of of Isatin 1a, L-proline 2, and Dipolarophiles 3[a]

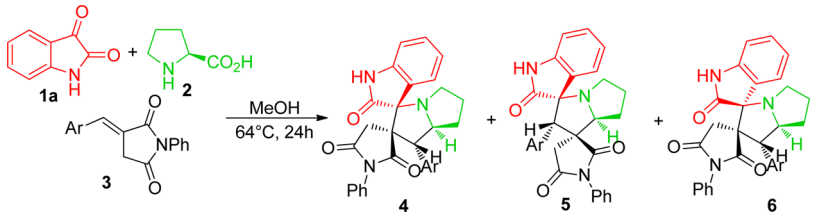

entry	Ar	products	yields (%)[b]	ratio[c] **4:5:6**
1	C_6H_5	**4a** + **5a** + **6a**	82	76:13:11
2	*p*-MeC_6H_4	**4b** + **5b** + **6b**	90	65:18:17
3	*p*-$MeOC_6H_4$	**4c** + **5c** + **6c**	92	71:18:11
4	*p*-ClC_6H_4	**4d** + **5d** + **6d**	85	53:28:19
5	*p*-FC_6H_4	**4e** + **5e** + **6e**	91	55:30:15

[a]The reactions were carried out with **1a** (0.5 mmol), **2** (0.75 mmol) and **3** (0.5 mmol) in methanol (10 mL) at 64 °C for 24 h. [b]Overall yields after isolation of the products by column chromatography. [c]Relative ratios were determined by ^{1}H NMR from the crude reaction mixture.

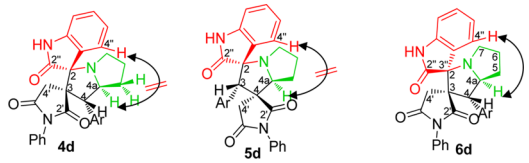

	4d	**5d**	**6d**
δH-4a ($J_{4a,5}$)	4.62-4.69	4.51 (4.9, 8.2)	4.20-4.28
δH-4 ($J_{4,4a}$)	4.05 (9.9)	-	5.05 (9.6)
δH-3	-	4.63	-
δH-4''	7.49	7.48	7.35

Figure 3. Selected ^{1}H NMR data (δ in ppm, J in Hz) and NOE correlations of isomers **4d**, **5d**, and **6d**.

multiplicity of these signals clearly demonstrate the regiochemistry of the cycloaddition reaction. In contrast, in the ^{1}H NMR spectra of regioisomer **5d** (Figure 3, middle) the pyrrolidinyl protons H-3 and H-4a appear as singlet resonating at δ 4.63 and as doublet of doublets at 4.51 ppm (J = 8.1 Hz, J = 4.9 Hz), respectively.

Comparison of the ^{1}H NMR spectra of **4d** and **6d** reveals two significant differences concerning the chemical shifts of the signals of H-4 and H-4a. The H-4 resonance in **4d** (4.05 ppm) is strongly upfield-shifted, with respect to the H-4 signal in **6d** (5.05 ppm), a rather unusual spectral region for a pyrrolidinyl proton. In contrast, the resonance of H-4a (4.62−4.69 ppm) in **4d** is shielded compared to that of **6d** (4.20−4.28 ppm). These effects can be attributed to the relative orientation of the carbonyl oxindole group attached to C-2. Thus, the NOESY spectra of **6d** (Figure S54 in Supporting Information (SI)) exhibits NOE contacts between H-4a and the aromatic proton H-4″ revealing that C-2″ and H-4a are in a *trans* relationship. The absence of NOE contacts between the aromatic proton H-4″ and H-4a in the NOESY spectra of **4d** and **5d** (Figure S52 and S53) indicates that C-2″ and H-4a are in *cis* relationship. The regio- and the stereochemical outcome of the cycloaddition was furthermore ascertained by X-ray analysis of the crystal structure of cycloadducts **4e**, **5d**, and **6d**, whose ORTEP presentations are shown in Figures S55−S57. The occurrence of interesting intra- and intermolecular hydrogen bonding in all three structures is discussed in detail in the SI and represented there in Figures S59−S61.

Discussion of the Reaction Mechanism. On the basis of our experimental results and previous studies on the reaction mechanism,[19] we propose in Scheme 3 a mechanistic pathway explaining the formation of **4** and **6** from the three-component reaction. The condensation of isatin **1a** with the amino acid **2** should lead to the formation of the two possible intermediates $\mathbf{I_1}$ and $\mathbf{I_{1'}}$. After the decarboxylation process, two different types of ylides can be formed: *W*-shaped $\mathbf{d_1}$ and *S*-shaped $\mathbf{d_{1'}}$

DOI: 10.1021/acs.joc.5b01399
J. Org. Chem. 2015, 80, 9064−9075

Scheme 2. Formation of Ylides d_1 and $d_{1'}$ as well as Their Possible Reaction with the Dipolarophile 3

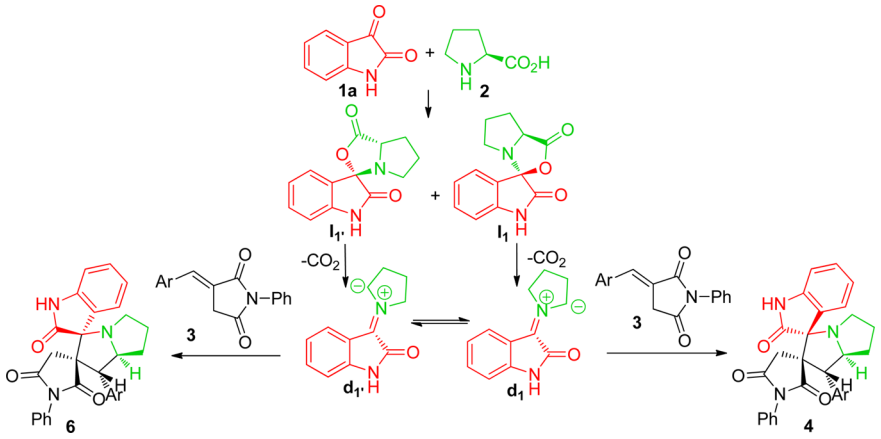

(Scheme 2). Experiments suggest that **4** and **6** result from the cycloaddition of $\mathbf{d_1}$ to the dipolarophile **3**. Hypothetically, the formation of product **6** could also involve the $\mathbf{d_{1'}}$ form (Scheme 2). However, this hypothesis was ruled out, since the formation of diastereoisomer **6** increased upon extending the reflux time of the reaction mixture and a total disappearance of the starting materials was finally observed (Table 1, entries 2 and 5).

Heating a solution of the major isomer **4** in methanol or acetonitrile for 4 h causes exclusive interconversion to product **6**. During this time, the competing formation of dipolarophile **1** is not observed (reaction monitored by TLC). Thus, we propose a ring-opening retro-Mannich reaction for the observed epimerization (Scheme 3). This mechanism has

Scheme 3. Proposed Mechanism Rationalizing the Formation of 5 and 6.

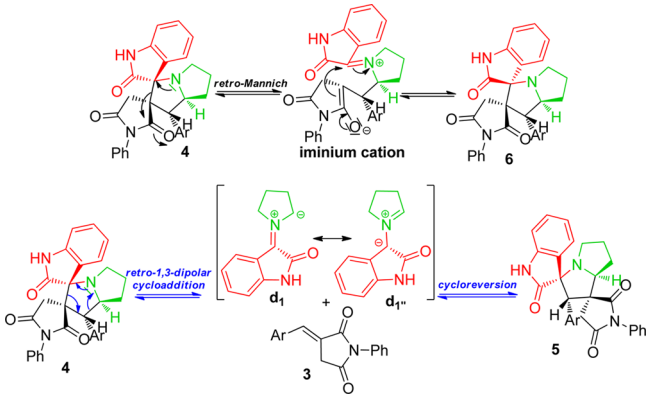

been suggested to explain isomerization in spirooxindole alkaloids[20] and pyrrolidine derivatives.[21] Interesting, when extending the reaction time to 24h under reflux, regioisomer **5** is formed after formation of the imide **1** as monitored by TLC. Thereby, the proposed mechanism for the formation of regioisomer **5** involves a retro-1,3-dipolar cycloaddition reaction to generate a *W*-shaped $\mathbf{d_{1''}}$ species, which then undergoes cycloreversion with the dipolarophile **3** through an *exo*-transition state (Scheme 3).

This result was totally unexpected having no precedent in the literature. Neither an example concerning the isomerization at the carbon of the spirooxindole core of related 1,3-dipolar adducts nor a retro-1,3-dipolar cycloaddition of spiropyrrolizidines was found. This tandem reaction is a straightforward route that allows access to a new isomeric class of spiropyrrolidizidines not accessible via direct 1,3-dipolar cycloaddition. All previously published studies showed that the cycloadducts were formed selectively through an *exo*-approach between the dipolarophile and the *W*-shaped ylide.

DFT Calculations. To enlighten the experimental results, and unveiling the regio- and stereoselectivity of these [3 + 2] cycloaddition, we conducted a DFT computational study. We chose to focus on the reaction of the dipolarophile **3d** with azomethine ylide $\mathbf{d_1}$. The stereochemistry of the cycloadducts is established by the ylide geometry and the *endo*/*exo* approach. Herein, we first explore the relative stability of the two possible isomers $\mathbf{d_1}$ and $\mathbf{d_{1'}}$ of the dipole-1,3 formed from the condensation of isatin **1a** with L-proline **2** (Scheme 1). In agreement with related literature,[18] the $\mathbf{d_1}$ form (*W*-shaped) is very slightly more stable than the $\mathbf{d_{1'}}$ form (*S*-shaped), by some 0.19 kcal·mol^{-1} (Scheme 4). Moreover, the attack of the

Scheme 4. Electronic Energies of Azomethine Ylides d_1 (*W*-shaped) and $d_{1'}$ (*S*-shaped) Calculated at the B3LYP/6-31G (d,p) level[a]

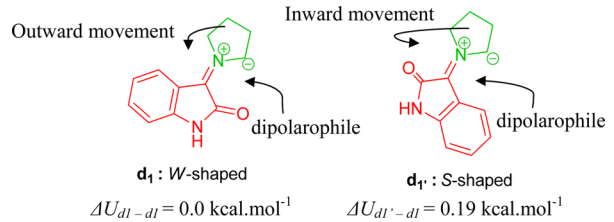

[a]The mode of the attack of the dipolarophile is also represented.

dipolarophile on $\mathbf{d_{1'}}$ should result in an unfavorable inward movement of the proline ring toward the isatin ring leading to the steric hindrance between these two fragments, while in the case of $\mathbf{d_1}$ a favorable outward movement can occur (Scheme 4).[22] Moreover, cycloadducts are always obtained from the *W*-shaped form and not from the *S*-shaped one.[17,18] Accordingly, calculations have been focused on the $\mathbf{d_1}$ conformation only.

A study using the frontier molecular orbital (FMO) model[23] was first carried out. An analysis of the HOMO−LUMO energy values (Table S1) indicates that the smaller energy difference is between HOMO ($\mathbf{d_1}$) and LUMO (**3d**) (ΔE = 0.12 eV), which predicts that the $HOMO_{dipole}$−$LUMO_{dipolarophile}$ interaction controls the cycloaddition reaction within a normal electron-demand reaction. The actual analysis of global and local

DOI: 10.1021/acs.joc.5b01399
J. Org. Chem. 2015, 80, 9064−9075

Scheme 5. Plausible Mechanism for the Regio- and Stereoisomeric 1,3-Dipolar Cycloaddition Reaction of Dipolarophile 3 with Azomethine Ylide d_1[a]

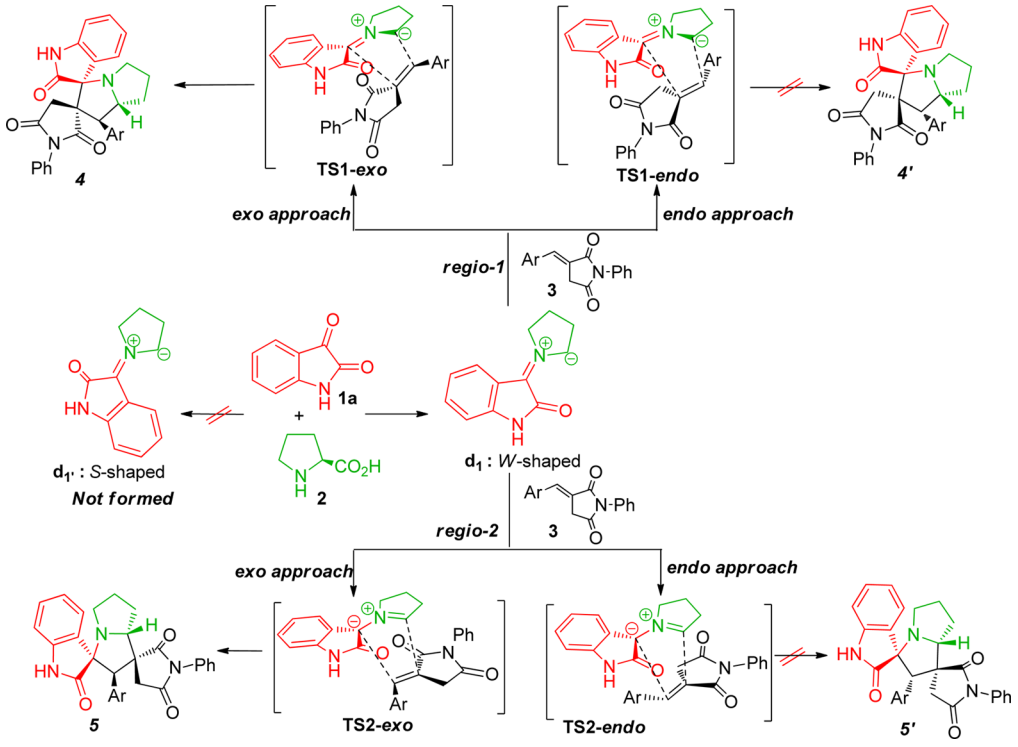

[a]Strike through arrows emphasize that the product is not experimentally obtained.

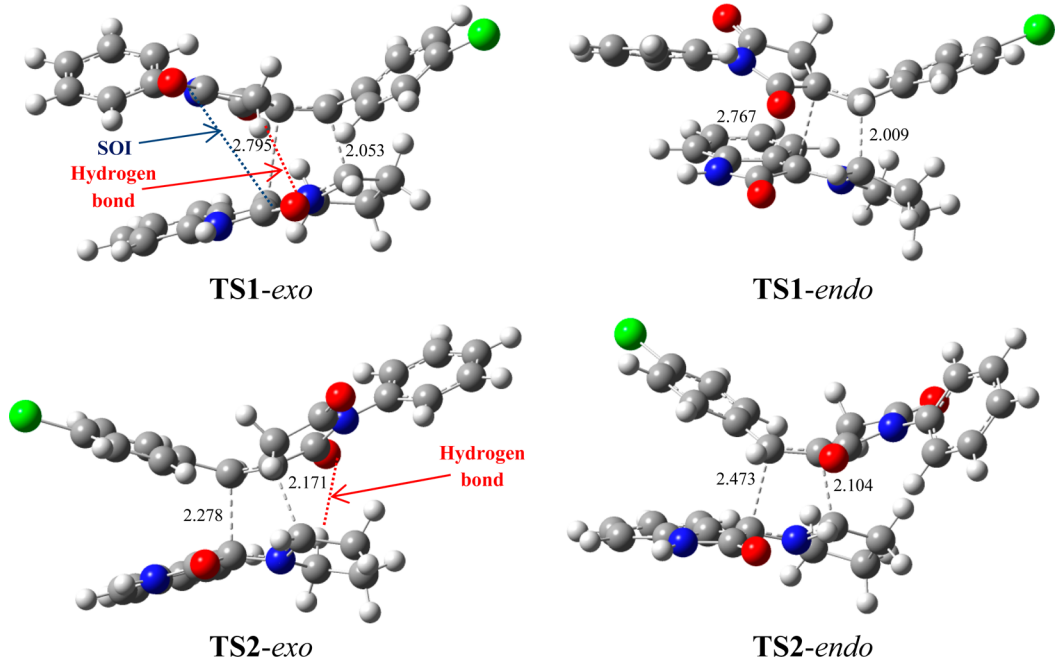

Figure 4. Four TS for the 1,3-dipolar cycloaddition of d_1 across **3d**, optimized at the B3LYP/6-31G(d,p) level. The lengths of the bonds directly involved in the reaction are given in Å.

properties is a powerful tool to understand the chemical reactivity of the system. Thus, electronic chemical potential μ, chemical hardness η, and global electrophilicity ω were calculated.

The electronic chemical potential μ describes the escaping tendency of electrons from an equilibrium system.[24] Its negative value is the absolute molecular electronegativity, χ. The chemical hardness η reveals the stability and reactivity of a chemical system.[22−25] The global electrophilicity ω measures the propensity or capacity of a species to accept electrons.[25g,26] Only relevant data are discussed in the present text. All the data are however presented in Table S1.

The computed electronic chemical potential of the ylide d_1 (μ = −3.320 eV) is higher than that of **3d** (μ = −4.462 eV), and

DOI: 10.1021/acs.joc.5b01399
J. Org. Chem. 2015, 80, 9064−9075

the chemical hardness of $\mathbf{d_1}$ (η = 2.204 eV) is lower than of **3d** (η = 2.231 eV), suggesting that the net charge transfer will take place from $\mathbf{d_1}$ toward **3d**. In addition, the electrophilicity of dipolarophile **3d** (ω = 4.462 eV) is greater than that of $\mathbf{d_1}$ (ω = 2.500 eV), indicating that the 1,3-dipole will act as a nucleophile, whereas **3d** will act as an electrophile.

The most favorable attack site can also be disclosed by theoretical calculations. The actual DFT-based local chemical reactivity Fukui function parameters for nucleophilic (f_k^+) and electrophilic (f_k^-) attacks were calculated through the electrostatic potential (ESP) derived atomic populations using eqs 1 and 2 respectively:[27]

$$f_k^+ = P_k^{N+1} - P_k^N = q_k^N - q_k^{N+1} \quad (1)$$

$$f_k^- = P_k^N - P_k^{N-1} = q_k^{N-1} - q_k^N \quad (2)$$

with k, N, P, and q, corresponding to the index of the atom, the number of electrons, the population number, and the net charge stemming from calculations, respectively. The calculated local chemical reactivity parameters of $\mathbf{d_1}$ and **3d** are shown Figure S1. The most favorable two-center interaction takes place between C-5 (possessing the highest value of f_k^- = 0.215) of the dipole $\mathbf{d_1}$ and C-4 (possessing the highest value of f_k^+ = 0.106) of the dipolarophile **3d**, leading primarily to the formation of the regioisomer **4d** which is in agreement with experimental observations (Table 2). In order to explain the formation of regioisomer **5d** in lower amount, the two regioisomeric pathways proposed in Scheme 5 have been studied. Four transition states (TS), TS1-*exo*-**4d**, TS1-*endo*-**4d**, TS2-*exo*-**5d**, and TS2-*endo*-**5d** were found to be associated with the two regioisomeric channels *endo*/*exo* stereoisomeric approach modes between the azomethine ylide $\mathbf{d_1}$ and the dipolarophile **3d**. Their cycloadducts were labeled **4d**, **4′d**, **5d**, and **5′d**. The TS are characterized by a saddle point with a single imaginary frequency. These TS are displayed in Figure 4. Kinetic and thermodynamic analyses can thus be carried out.

Differences in the Gibbs free energy (ΔG), enthalpy (ΔH), and entropy (ΔS) for the different stationary points along the reactive pathways are reported in Table S2. All the energy values have been corrected for the zero point energy. The kinetic parameters (activation energy, activation enthalpies, and activation entropies between reactants and TS) are first discussed. The energy requested to reach the TS, i.e., the activation energy, was shown to increase in the following order: **TS1**-*exo* < **TS2**-*exo* < **TS1**-*endo* < **TS2**-*endo*. The *exo* approach was found to be highly favored over the *endo* approach. The most favorable pathway, via the **TS1**-*exo*, exhibits a significantly lower activation energy (21.0 kcal·mol^{-1}) than that stemming from the second most probable route via the **TS2**-*exo* (25.3 kcal·mol^{-1}). The favored *exo* approaches compared with the *endo* attack fit experimental conclusions showing that mixtures of the two *exo*-regioisomeric are only observed.

The close similarity between the four activation entropies, ranging from −48.1 to −51.8 cal mol^{-1} K^{-1}, highlights that reactions are enthalpy driven. From an energetic point of view, structural investigation (Figure 4) of these TS reveals that the dipole and dipolarophile are largely superimposed in the **TS1**-*exo*. Thus, the significantly lowest activation energy value of **TS1**-*exo* among the four TS can be partially explained by secondary orbital interactions (SOI)[28] that occur between the oxygen atom of the carbonyl of isatin and the carbon atom of the carbonyl of the dipolarophile. Moreover, an additional hydrogen bond is formed in **TS1**-*exo* between one of the methylene hydrogen atoms of dipolarophile **3d** with the carbonyl of the azomethine ylide $\mathbf{d_1}$ (2.430 Å). On the other hand, **TS2**-*exo* is only stabilized by a hydrogen bond that occurs between one of the methylene hydrogen atoms of the proline ring of the azomethine ylide with carbonyl of dipolarophile **3d** (2.453 Å).[15b,29] Thermodynamic analysis of the studied reactions can now be investigated. ΔG, ΔH, and ΔS between reactants and products were also computed. The lowest ΔG values are achieved in the *exo* approach on **5d** and **4d** (0.5 and 1.2 kcal·mol^{-1}, respectively). Similarly to the activation entropies, ΔS for these cycloadditions are found negative, and their values were comparable, in the range of −51.6 to −54.8 cal K^{-1} mol^{-1}. The *exo* approach unveils slightly more negative values than those corresponding to the *endo* one. Thus, the reactions are also enthalpy driven. Moreover, all cycloadditions are exothermic processes, and ΔH is in the range of −5.6 to −15.4 kcal·mol^{-1}. It is worth noting that in the gas phase, calculations predict that these reactions have positive free Gibbs energies ($\Delta G > 0$). Conversely, the experimental results in methanol showed that the reaction is spontaneous toward the products. The issue of these negative values for the free Gibbs enthalpy is the subject of forthcoming studies dealing with the presence of solvent. Nevertheless, these negative values suggest that this reaction is mainly kinetic dependent. Accordingly, thanks to DFT investigation, the most favorable pathway is established. It goes through **TS1**-*exo* (**4d**) and **TS2**-*exo* (**5d**) under kinetic control, with **4d** being slightly more stable than **5d**. This conclusion is in perfect accordance with the experimental observation assigning the *exo*-regioisomer **4d** as the major formed product, whereas **5d** is the minor one.

All the TS are concerted asynchronous as expected for a typical normal-demand 1,3-dipolar cycloaddition. To support this accordance, the two new bonds lengths are measured. At the TS associated with the regioisomeric channels 1 (Figure 4), the length of the C-2−C-3 forming bonds are 2.767 Å at **TS1**-*endo* and 2.795 Å at **TS1**-*exo*, while the distance between the C-4a and the C-4 atoms is 2.009 Å at **TS1**-*endo* and 2.053 Å at **TS1**-*exo*. At the TSs associated with the regioisomeric channels 2 (Figure 4), the length of the C-2−C-3 forming bonds is 2.473 Å at **TS2**-*endo* and 2.278 Å at **TS2**-*exo*, while the distance between the C-4a and the C-4 atoms is 2.104 Å at **TS2**-*endo* and 2.171 Å at **TS2**-*exo*. The extent of the asynchronicity of the bond-formation can thus be measured by the difference between the lengths of the two σ bonds being formed in the reaction, i.e., $\Delta d = l_1 - l_2$. The asynchronicity at the regioisomeric channel 1 is Δd = 0.75 Å at **TS1**-*endo* and 0.74 Å at **TS1**-*exo*, while that at the regioisomeric channel 2 is Δd = 0.37 Å at **TS2**-*endo* and 0.10 Å at **TS2**-*exo*. Therefore, the formation of the TS associated with channel 1 is favored. Accordingly, DFT investigation is in perfect agreement with the experimental observation assigning the *exo*-regioisomer **4d** as the major formed product.

Synthesis of the Spiropyrrolizidines 7 and Piperazine 8. Encouraged by these results, we examined the regio- and stereoselectivity of the three-component 1,3-dipolar cycloaddition reaction of the dipolarophile **3**, L-proline with other cyclic diketones such as indenoquinoxaline-11-one **1b** and acenaphthenequinone **1c** (Scheme 6). When the reaction was investigated with **1b** in MeOH as reaction medium, the spiropyrrozolidines **7a−c** were obtained in good yields as sole stereoisomers (Table 3, entries 1−3). Surprisingly, the use of

DOI: 10.1021/acs.joc.5b01399
J. Org. Chem. 2015, 80, 9064−9075

Scheme 6. Reaction of (*E*)-3-Arylidene-1-phenyl-pyrrolidine-2,5-diones 3, L-Proline with Cyclic Ketones 1b and 1c

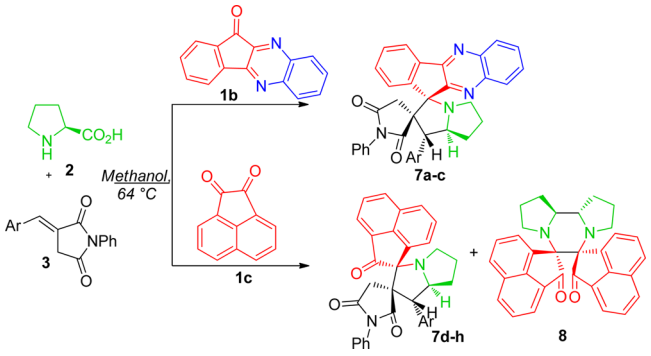

Table 3. Synthesis of Dispiropyrrolizidine Derivatives 7 and Piperazine 8

entry	diketone	Ar	products	ratio[a] 7:8
1	**1b**	*p*-MeC_6H_4	**7a**	100:00
2	**1b**	*p*-$MeOC_6H_4$	**7b**	100:00
2	**1b**	*p*-ClC_6H_4	**7c**	100:00
4	**1c**	C_6H_5	**7d** + **8**	70:30
5	**1c**	*p*-MeC_6H_4	**7e** + **8**	67:33
6	**1c**	*p*-$MeOC_6H_4$	**7f** + **8**	62:38
7	**1c**	*p*-ClC_6H_4	**7g** + **8**	75:25
8	**1c**	*p*-BrC_6H_4	**7h** + **8**	80:20

[a]Isolated yield after purification by column chromatography. [b]Relative ratios were determined by ^{1}H NMR from the crude reaction with **1c**.

1c as reaction component in the cycloaddition led, along with the formation the spiropyrrolizidine derivatives **7d–h**, to creation of the fused piperazine **8**, a dimer of the 1,3-dipole (Table 3, entries 4–8).

Synthesis and Characterization of Fused Piperazines 8. To the best of our knowledge, the lock and key chemistry of the dimerization of an azomethine ylide derived from acenaphthenequinone **1c** and L-proline **2** was not yet documented in the literature. However, some articles reported the synthesis of the [3 + 3] cycloaddition (dimerization) of the azomethine ylide stemming from condensation of isatin **1a** and L-proline **2**.[30] We were thus interested in the dimerization reaction of $\mathbf{d_2}$ as tool for building novel dispiro-acenaphthenones. These reagents, admixed together without any dipolarophile, afforded two compounds after 2 h in refluxing methanol (Scheme 7). After separation by column chromatography, they were identified as dimer **8** and its regioisomer **9** in a 70:30 ratio. Structural elucidation of these compounds **8** and **9** was accomplished using the NMR spectroscopic data and a single-crystal X-ray diffraction study. In the ^{1}H NMR spectra, six aromatic protons were found, followed by seven protons in the aliphatic region, indicating that these molecules are symmetric. In the hypothetical case of formation of the alternative isomers **8′** and **9′** (Scheme 7), the observation of the twice number of protons in the aliphatic and aromatic regions would be expected. Since **8** and **9** are difficult to distinguish by NMR spectroscopy, we therefore characterized piperazine **8** by means of a single-crystal X-ray diffraction study, whose his ORTEP is shown in Figures S58.

Scheme 7. Proposed Dimerization Mechanism of Azomethine Ylides $\mathbf{d_2}$ and $\mathbf{d_{2'}}$

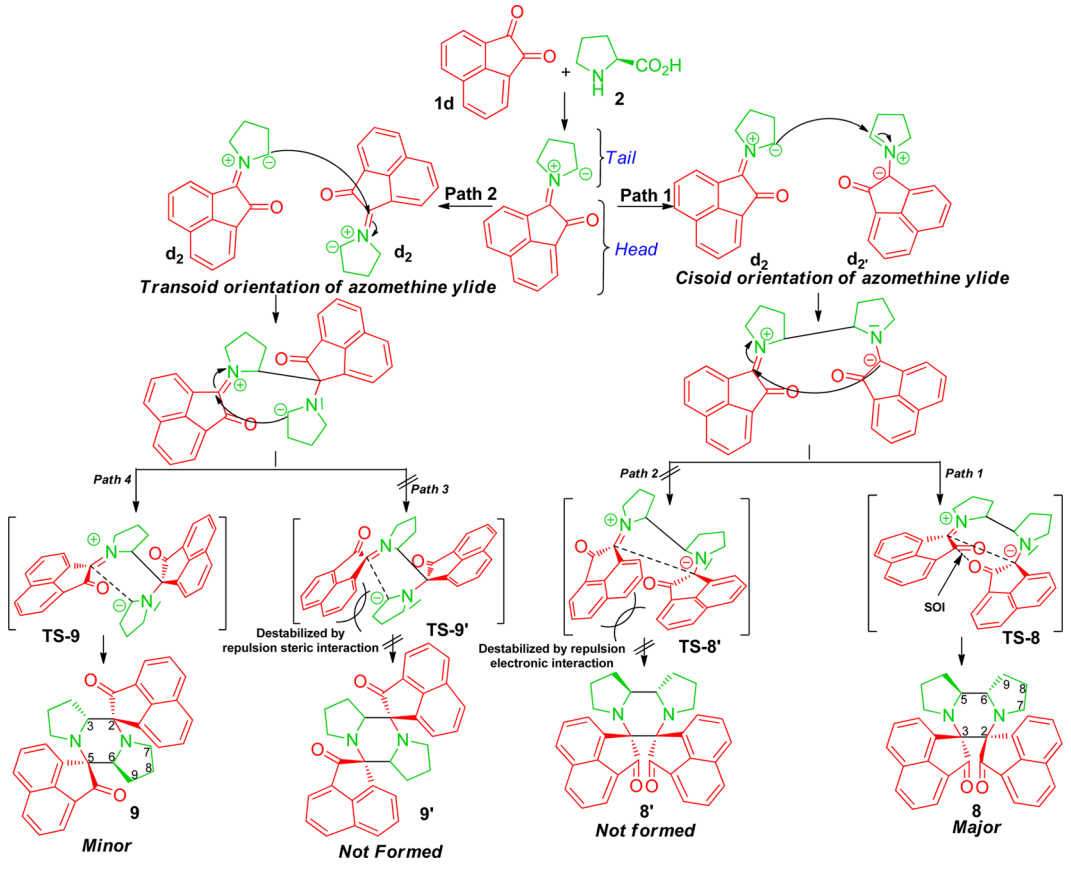

DOI: 10.1021/acs.joc.5b01399
J. Org. Chem. 2015, 80, 9064–9075

To explain the reaction mechanism, it should be noted that the dipole presents two mesomeric forms $\mathbf{d_2}$ and $\mathbf{d_{2'}}$. Thus, two pathways are possible: the first one occurring in a head−head fashion of $\mathbf{d_2}$ + $\mathbf{d_{2'}}$ leading to the formation of compounds **8** and **8′**; the second consisting of the cycloaddition by a head−tail way of $\mathbf{d_2}$ + $\mathbf{d_2}$ giving the dispiro-acenaphthenones **9** and **9′**. The observed regioselectivity can be explained based on the TS depicted in Scheme 7. In fact, the possible path 2 led to repulsive electronic interaction between the two acenaphthenone cores of $\mathbf{d_2}$ and $\mathbf{d_{2'}}$ in **TS-8′**. Furthermore, **TS-9′** presents electrostatic repulsion between the pyrrolidine residue and the acenaphthenone moiety of $\mathbf{d_2}$ (path 3). For these reasons, formation of dimers **8′** and **9′** is unfavorable. However, the **TS-8** leading to product **8** (path 1) is the more favorable and predominant due to a SOI between the orbital of the carbonyl group of $\mathbf{d_2}$ with those of the ylide $\mathbf{d_{2'}}$ (ratio of **8**:**9** is 70:30).

CONCLUSION

We reported the synthesis of a very new series of spiropyrrolizidine derivatives via a three-component 1,3-dipolar cycloaddition reaction of (*E*)-3-arylidene-1-phenyl-pyrrolidine-2,5-diones, L-proline, and cyclic ketones isatin, indenoquinoxaline-11-one, and acenaphthenequinone. We showed that spirooxindolepyrrolizidine undergoes a reversible ring opening cyclization reaction affording a new family of compounds with unusual relative stereochemistry. Furthermore, these cycloadducts undergo retro-1,3-dipolar cycloaddition yielding an unexpected regioisomers. An analysis based on theoretical calculations using the DFT approach at the B3LYP/6-31G(d,p) level revealed that the spirocycloadduct **4** is obtained through a 1,3-dipolar cycloaddition reaction via a high asynchronous mechanism with a very low activation energy, as compared to the other possible reaction paths. This outcome is in agreement with the experimental observations. Another important highlight of the present work is the isolation of polycyclic fused piperazines, stemming from reaction of the dipolarophiles with azomethine ylides derived from condensation of acenaphthenequinone and L-proline. This methodology implying a stepwise [3 + 3] cycloaddition pathway was further developed allowing to access new dispiropiperazine-containing compounds. These compounds were fully characterized for the first time in literature. The biological activities of our spiropyrrolizidine derivatives will be investigated. We intend also to perform calculations on the [3 + 3] cycloaddition using the DFT approach.

EXPERIMENTAL SECTION

General Experimental Methods. NMR spectra were recorded on a 300 MHz spectrometer operating at 75 MHz for the ^{13}C NMR spectra. Chemical shifts are reported in ppm with the solvent resonance as the internal standard ($CDCl_3$: δ 7.26 ppm in ^{1}H NMR and δ 75.00 ppm in ^{13}C NMR). The following abbreviations were used to explain the multiplicities: bs = broad singlet, s = singlet, d = doublet, dd = doublet of doublets, m = multiplet. IR spectra were recorded in the ATR mode. Elemental analyses were performed on a CHNS-elemental analyzer. Materials: thin-layer chromatography (TLC): TLC plates (silica gel 60 F_{254} 0.2 mm 200 × 200 nm); substances were detected using UV light at 254 nm. The (*E*)-3-arylidene-1-phenyl-pyrrolidine-2,5-diones **3a−e** were prepared by Wittig reaction between *N*-phenyl maleimide and aromatic aldehyde.[31]

General Procedure for the Preparation of Cycloadducts 4−6. A mixture of **3** (0.5 mmol), L-proline **2** (0.75 mmol), and isatin **1a** or acenaphthenequinone **1b** was refluxed in methanol (10 mL) for 24 h. After completion of the reaction as monitored from TLC, the solvent was removed under reduced pressure, and residue was chromatographed on silica gel employing ethyl acetate-cyclohexane (3:7 v/v) as eluent to obtain the pure products **4−6**.

Spiro[2,3″]oxindole-spiro-[3,3′]-*N*-phenylsuccinimide-4-phenylhexahydro-1*H*-pyrrolizine 4a. White solid (144 mg, 82%); mp 177−178 °C; ^{1}H NMR δ (ppm): 8.93 (bs, 1H), 6.81−7.57 (m, 14H), 4.73−4.78 (m, 1H), 4.16 (d, J = 9.9 Hz, 1H), 3.30−3.42 (m and d,, J = 18.9 Hz, 2H), 2.79−2.85 (m, 1H), 2.71 (d, J = 18.9 Hz, 1H), 1.97−2.19 (m, 3H), 1.42−1.81 (m, 1H); ^{13}C NMR δ 178.1, 177.2, 173.2, 140.8, 135.7, 131.1, 129.5, 129.1, 128.6, 128.4, 128.0, 127.9, 127.4, 125.9, 124.6, 121.8, 110.1, 76.9, 67.8, 64.8, 56.7, 47.0, 35.2, 29.5, 26.4; IR ν 3225, 1778, 1707 cm^{-1}; Anal. calcd for $C_{29}H_{25}N_3O_3$: C, 75.14; H, 5.44; N, 9.07; found: C, 75.18; H, 5.45; N, 8.98.

Spiro[2,3″]oxindole-spiro-[3,3′]-*N*-phenylsuccinimide-4-(4-methylphenyl)hexahydro-1*H*-pyrrolizine 4b. White solid (139 mg, 90%); mp 240−241 °C; ^{1}H NMR δ (ppm): 8.96 (bs, 1H), 6.86−7.60 (m, 13H), 4.73−4.77 (m, 1H), 4.15 (d, J = 10.2 Hz, 1H), 3.42 (d, J = 18.7 Hz, 1H), 3.33−3.35 (m, 1H), 2.80−2.85 (m, 1H), 2.75 (d, J = 18.7 Hz, 1H), 2.38 (s, 3H), 2,02−2.20 (m, 3H), 1.81−2.20 (m, 1H); ^{13}C NMR δ 178.1, 177.2, 173.3, 140.8, 137.1, 132.5, 131.2, 129.4, 128.9, 128.3, 128.0, 127.9, 125.9, 124.7, 121.8, 110.1, 76.8, 67.7, 64.8, 56.4, 46.9, 35.1, 29.5, 26.4, 20.4; IR ν 3247, 1787, 1708 cm^{-1}; Anal. calcd for $C_{30}H_{27}N_3O_3$: C, 75.45; H, 5.70; N, 8.80; found: C, 75.41; H, 5.67; N, 8.75.

Spiro[2,3″]oxindole-spiro-[3,3′]-*N*-phenylsuccinimide-4-(4-methoxyphenyl)hexahydro-1*H*-pyrrolizine 4c. White solid (160 mg, 92%); mp 232−233 °C; ^{1}H NMR δ (ppm): 8.92 (bs, 1H), 6.84−7.58 (m, 13H), 4.80 (m, 1H), 4.11 (d, J = 9.9 Hz, 1H), 3.83 (s, 3H), 3.33−3.43 (d and m, J = 18.7 Hz, 2H), 2.83 (m, 1H), 2.75 (d, J = 18.7 Hz, 1H), 1,99−2.20 (m, 3H), 1.78−1.82 (m, 1H); ^{13}C NMR δ 177.7, 173.9, 159.3, 141.2, 130.6, 130.1, 128.9, 128.5, 128.5, 126.4, 122.4, 114.7, 114.5, 110.7, 76.6, 68.4, 65.1, 56.6, 55.2, 47.6, 35.6, 30.0, 26.9; IR ν 3222, 1787, 1708 cm^{-1}; Anal. calcd for $C_{30}H_{27}N_3O_4$: C, 73.01; H, 5.51; N, 8.51; found: C, 73.09; H, 5.45; N, 8.46.

Spiro[2,3″]oxindole-spiro-[3,3′]-*N*-phenylsuccinimide-4-(4-chlorophenyl)hexahydro-1*H*-pyrrolizines 4d. White solid (111 mg, 85%); mp 213-214 °C; ^{1}H NMR δ (ppm): 8.41 (bs, 1H), 6.76−7.50 (m, 13H), 4.62−4.69 (m, 1H), 4.05 (d, J = 9.9 Hz, 1H), 3.32−3.41 (m, 1H), 3.23 (d, J = 18.7 Hz, 1H), 2.75−2.81 (m, 1H), 2.60 (d, J = 18.7 Hz, 1H), 1.89−2.18 (m, 3H), 1.70−1.79 (m, 1H); ^{13}C NMR δ 178.1, 178.0, 173.7, 141.1, 134.9, 133.9, 131.4, 131.1, 130.2, 129.5, 129.3, 129.1, 129.0, 128.6, 128.4, 126.4, 122.6, 110.5, 76.6, 68.9, 65.1, 57.0, 47.6, 36.1, 29.9, 26.3; IR ν 3266, 1771, 1706 cm^{-1}; Anal. calcd for $C_{29}H_{24}ClN_3O_3$: C, 69.95; H, 4.86; N, 8.44; found: C, 70.00; H, 4.94; N, 8.50.

Spiro[2,3″]oxindole-spiro-[3,3′]-*N*-phenylsuccinimide-4-(4-fluorophenyl)hexahydro-1*H*-pyrrolizine 4e. White solid (120 mg, 91%); mp 216−217 °C; ^{1}H NMR δ (ppm): 8.45 (bs, 1H), 6.83−7.56 (m, 13H), 4.67−4.74 (m, 1H), 4.12 (d, J = 10.2 Hz, 1H), 3.36−3.44 (m, 1H), 3.29 (d, J = 18.6 Hz, 1H), 2.79−2.85 (m, 1H), 2.41 (d, J = 18.6 Hz, 1H), 1.96−2.19 (m, 3H), 1.73−1.84 (m, 1H); ^{13}C NMR δ 177.7, 177.5, 173.0, 160.3, 140.7, 131.7, 131.6, 131.1, 130.8, 130.7, 129.6, 128.3, 128.0, 125.8, 124.5, 121.9, 115.6, 115.3, 109.9, 76.4, 68.4, 64.7, 56.4, 47.0, 35.5, 29.3, 25.8; IR ν 3198, 1777, 1702 cm^{-1}; Anal. calcd for $C_{29}H_{24}FN_3O_3$: C, 72.34; H, 5.02; N, 8.73; found: C, 72.26; H, 5.08; N, 8.77.

Spiro[2,3″]oxindole-spiro-[4,3′]-*N*-phenylsuccinimide-3-phenylhexahydro-1*H*-pyrrolizines 5a. White solid (25 mg, 82%); mp170−171 °C; ^{1}H NMR δ (ppm): 7.81 (bs, 1H), 6.74−7.71 (m, 14H), 5.29 (s, 1H), 4.60 (dd, J = 8.1 Hz, J = 5.1 Hz, 1H), 3.21−3.34 (d and m, J = 18.9 Hz, 2H), 3.13 (d, J = 18.9 Hz, 1H), 2.74−2.78 (m, 1H), 1.87−2.22 (m, 4H); ^{13}C NMR δ 179.9, 178.2, 174.4, 140.9, 133.0, 131.6, 131.5, 129.1, 129.0, 128.5, 128.4, 127.9, 127.8, 127.3, 126.1, 125.9, 125.1, 121.9, 109.3, 74.9, 73.8, 58.3, 56.4, 48.7, 41.2, 27.0, 25.0, IR ν 3228, 1780, 1707 cm^{-1}; Anal. calcd for $C_{29}H_{25}N_3O_3$: C, 75.14; H, 5.44; N, 9.07; found: C, 75.25; H, 5.36; N, 9.16.

Spiro[2,3″]oxindole-spiro-[4,3′]-*N*-phenylsuccinimide-3-(4-methylphenyl)hexahydro-1*H*-pyrrolizines 5b. White solid (38 mg, 90%); mp 235−236 °C; ^{1}H NMR δ (ppm): 7.60 (bs, 1H), 6.75−7.49 (m, 13H), 4.74 (s, 1H), 4.60 (dd, J = 7.8 Hz, J = 4.8 Hz, 1H),

DOI: 10.1021/acs.joc.5b01399
J. Org. Chem. 2015, 80, 9064−9075

3.21−3.35 (d and m, J = 18.6 Hz, 2H), 3.15 (d, J = 18.6 Hz, 1H), 2.75−2.80 (m, 1H), 1.85−2.24 (m and s, 7H); ^{13}C NMR δ 180.4, 178.6, 175.0, 141.4, 137.5, 130.3, 129.6, 129.4, 129.0, 128.4, 126.4,125.6, 122.4, 109.7, 77.1, 75.3, 74.3, 58.8, 56.6, 49.2, 41.7, 27.5, 25.4,20.8; IR ν 3249, 1787, 1710 cm^{-1}; Anal. calcd for $C_{30}H_{27}N_3O_3$: C, 75.45; H, 5.70; N, 8.80; found: C, 75.37; H, 5.79; N, 8.91.

Spiro[2,3″]oxindole-spiro-[4,3′]-*N*-phenylsuccinimide-3-(4-methoxyphenyl)hexahydro-1*H*-pyrrolizines 5c. White solid (40 mg, 92%); mp 223−224 °C; ^{1}H NMR δ (ppm): 7.84 (bs, 1H), 6.65−7.48 (m, 13H), 4.69 (s, 1H), 4.58 (dd, J = 8.1 Hz, J = 4.8 Hz, 1H), 3.67 (s 3H), 3.21−3.30 (m and d, J = 18.9 Hz, 2H), 3.15 (d, J = 18.9 Hz, 1H), 2.76−2.78 (m, 1H),1.88−2.18 (m, 4H); ^{13}C NMR δ 180.5, 179.1, 175.2, 159.1, 141.3, 130.7, 129.6, 129.1, 128.5, 126.6, 126.4, 125.6, 122.5, 114.3, 109.9, 77.2, 75.2, 74.5, 58.8, 55.0, 49.4, 41.7, 27.5, 25.5; IR ν 3221, 1789, 1709 cm^{-1}; Anal. calcd for $C_{30}H_{27}N_3O_4$: C, 73.01; H, 5.51; N, 8.51; found: C, 73.07; H, 5.58; N, 8.47.

Spiro[2,3″]oxindole-spiro-[4,3′]-*N*-phenylsuccinimide-3-(4-chlorophenyl)hexahydro-1*H*-pyrrolizine 5d. White solid (59 mg, 85%); mp 189−190 °C; ^{1}H NMR δ (ppm): 7.86 (bs, 1H), 6.69−7.42 (m, 13H), 4.63 (s, 1H), 4.51 (dd, J = 8.1 Hz, J = 4.8 Hz, 1H), 3.17−3.24 (d and m, J = 18.7, 2H), 3.00 (d, J = 18.7 Hz, 1H), 2.66−2.71 (m, 1H), 2.09−2.16 (m, 1H), 1.75−1.97 (m, 3H); ^{13}C NMR δ 180.2, 178.7, 174.8, 141.3, 134.0, 131.9, 131.9, 131.0, 129.9, 129.2, 129.1, 128.6, 126.4, 126.2, 125.6, 122.6, 110.1, 75.5, 74.5, 58.8, 55.9, 49.4, 41.7, 27.6, 25.5; IR ν 3264, 1770, 1706 cm^{-1}; Anal. calcd for $C_{29}H_{24}ClN_3O_3$: C, 69.95; H, 4.86; N, 8.44; found: C, 70.01; H, 4.97; N, 8.55.

Spiro[2,3″]oxindole-spiro-[4,3′]-*N*-phenylsuccinimide-3-(4-fluorophenyl)hexahydro-1*H*-pyrrolizine 5e. White solid (65 mg, 91%); mp 197−198 °C; ^{1}H NMR δ (ppm): 7.86 (bs, 1H), 6.69−7.42 (m, 13H), 4.63 (s, 1H), 4.51 (dd, J = 8.1 Hz, J = 4.8 Hz, 1H), 3.17−3.24 (d and m, J = 18.7 Hz, 2H), 3.00 (d, J = 18.7 Hz, 1H), 2.66−2.71 (m, 1H), 2.09−2.16 (m, 1H), 1.75−1.97 (m, 3H); ^{13}C NMR δ 180.0, 178.4, 174.9, 141.6, 131.4, 131.3, 129.1, 128.5, 126.3, 125.6, 122.5, 116.0, 115.8, 110.2, 75.6, 74.3, 58.6, 55.9, 49.4, 41.5, 27.7, 25.6; IR ν 3205, 1778, 1704 cm^{-1}; Anal. calcd for $C_{29}H_{24}FN_3O_3$: C, 72.34; H, 5.02; N, 8.73; found: C, 72.40; H, 4.99; N, 8.79.

Spiro[2,3″]oxindole-spiro-[3,3′]-*N*-phenylsuccinimide-4-phenylhexahydro-1*H*-pyrrolizine 6a. White solid (21 mg, 82%); mp 190−191 °C; ^{1}H NMR δ (ppm): 7.72 (bs, 1H), 6.64−7.49 (m, 14H), 5.06 (d, J = 9.6 Hz, 1H), 4.29−4.32 (m, 1H), 3.38 (d, J = 18.1 Hz, 1H), 2.87 (d, J = 18.1 Hz, 1H), 2.72−2.74 (m, 2H), 2.05−2.26 (m, 4H); ^{13}C NMR δ 178.4, 175.8, 173.5, 141.3, 135.9, 131.2, 130.1, 129.1, 129.0, 128.9, 128.8, 128.8, 128.6, 128.5, 127.8, 126.3, 126.1, 122.5, 110.0, 77.4, 66.3, 66.0, 49.6, 47.4, 34.2, 30.0; IR ν 3279, 1772, 1725, cm^{-1}; Anal. calcd for $C_{29}H_{25}N_3O_3$: C, 75.14; H, 5.44; N, 9.07; found: C, 75.23; H, 5.52; N, 9.01.

Spiro[2,3″]oxindole-spiro-[3,3′]-*N*-phenylsuccinimide-4-(4-methylphenyl)hexahydro-1*H*-pyrrolizine 6b. White solid (37 mg, 90%); mp 164−165 °C; ^{1}H NMR δ (ppm): 6.68−7.50 (m, 14H), 5.03 (d, J = 9.9 Hz, 1H), 4.27 (m, 1H), 3.37 (d, J = 18.1 Hz, 1H), 2.89 (d, J = 18.1 Hz, 1H), 2.76 (m, 2H), 2.33 (s, 3H), 2.05−2.28 (m, 4H); ^{13}C NMR δ 178.3, 174.8, 173.5, 141.2, 137.5, 132.7, 131.3, 130.0, 129.6, 128.9, 128.5, 126.3, 122.4, 109.8, 77.9, 66.3, 66.0, 58.4, 49.3, 47.4, 34.2, 30.0, 21.0; IR ν 3251, 1786, 1720 cm^{-1}; Anal. calcd for $C_{30}H_{27}N_3O_3$: C, 75.45; H, 5.70; N, 8.80; found: C, 75.52; H, 5.61; N, 8.87.

Spiro[2,3″]oxindole-spiro-[3,3′]-*N*-phenylsuccinimide-4-(4-methoxyphenyl)hexahydro-1*H*-pyrrolizines 6c. White solid (26 mg, 92%); mp 182−183 °C; ^{1}H NMR δ (ppm): 6.71−7.54 (m, 14H), 5.01 (d, J = 9.6 Hz, 1H), 4.26−4.29 (m, 1H), 3.82 (s, 3H), 3.38 (d, J = 18 Hz, 1H), 2.91 (d, J = 18 Hz, 1H), 2.76−2.78 (m, 2H), 2.30 (m, 1H), 2.07 (m, 3H); ^{13}C NMR δ 180.0, 175.2, 174.5, 159.5, 140.3, 132.1, 129.7, 129.4, 129.1, 128.7, 128.3, 126.2, 122.4, 114.4, 77.9, 66.1, 58.3, 55.2, 49.2, 34.1, 30.7, 29.8; IR ν 3230, 1787, 1723 cm^{-1}; Anal. calcd for $C_{30}H_{27}N_3O_4$: C, 73.01; H, 5.51; N, 8.51; found: C, 72.94; H, 5.42; N, 8.61.

Spiro[2,3″]oxindole-spiro-[3,3′]-*N*-phenylsuccinimide-4-(4-chlorophenyl)hexahydro-1*H*-pyrrolizine 6d. White solid (41 mg, 85%); mp 228−229 °C; ^{1}H NMR δ (ppm): 7.65 (bs, 1H), 6.63−7.50 (m, 13H), 5.05 (d, J = 9.6 Hz, 1H), 4.20−4.28 (m, 1H), 3.39 (d, J = 18.1 Hz, 1H), 2.70−2.83 (m and d, J = 18.1 Hz, 3H), 2.25−2.27 (m, 1H), 2.00−2.16 (m, 3H); ^{13}C NMR δ 178.1, 174.7, 173.1, 143.9, 134.5, 133.7, 131.2, 130.1, 130.0, 129.1, 128.9, 128.6, 126.2, 126.0, 122.5, 110.0, 78.0, 66.3, 65.9, 48.7, 47.4, 34.1, 30.7, 30.0; IR ν 3264, 1772, 1715 cm^{-1}; Anal. calcd for $C_{29}H_{24}ClN_3O_3$: C, 69.95; H, 4.86; N, 8.44; found: C, 70.03; H, 4.95; N, 8.33.

Spiro[2,3″]oxindole-spiro-[3,3′]-*N*-phenylsuccinimide-4-(4-fluorophenyl)hexahydro-1*H*-pyrrolizine 6e. White solid (33 mg, 91%); mp 230−231 °C; ^{1}H NMR δ (ppm): 7.71 (bs, 1H), 6.66−7.50 (m, 13H), 5.07 (d, J = 9.6 Hz, 1H), 4.21−4.27 (m, 1H), 3.40 (d, J = 18 Hz, 1H), 2.71−2.86 (m and d, J = 18 Hz, 3H), 2.24−2.28 (m, 1H), 2.01−2.12 (m, 3H); ^{13}C NMR δ 178.3, 174.7, 173.0, 160.6, 141.3, 131.7, 131.3, 130.3, 130.2, 130.1, 128.9, 128.5, 126.4, 126.2, 122.5, 116.0, 115.7, 109.9, 78.0, 66.5, 65.9, 48.9, 47.4, 34.1, 30.7, 29.9; IR ν 3200, 1779, 1715 cm^{-1}; Anal. calcd for $C_{29}H_{24}FN_3O_3$: C, 72.34; H, 5.02; N, 8.73; found: C, 72.42; H, 4.95; N, 8.78.

General Procedure for the Preparation of Spiro-indenoquinoxaline Pyrrolizidines 7a−c. A mixture of ninhydrin (0.5 mmol) and 1,2-phenylenediamine (0.5 mmol) and L-proline **2** (0.5 mmol) was stirred for 10 min in 10 mL of methanol, followed by the addition of dipolarophile **3** (0.5 mmol). The mixture was then refluxed for 4 h until completion of the reaction as evidenced by TLC. The solvent was removed under reduced pressure, and the crude product obtained was purified by column chromatography on silica gel using ethyl acetate-cyclohexane (3:7 v/v) as eluent to provide the pure product **7a−c**.

Spiro[2,11″]indeno-[1,2b]-quinoxaline-spiro-[3,3′]-*N*-phenylsuccinimide-4-(4-methylphenyl)hexahydro-1*H*-pyrrolizines 7a. Yellow solid (197 mg, 70%); mp 209−210 °C; ^{1}H NMR δ (ppm): 6.52−8.27 (m, 17H), 4.79−4.87 (m, 1H), 4.51 (d, J = 10.2 Hz, 1H), 4.14 (d, J = 18.3 Hz, 1H), 2.87−2.96 (m, 1H), 2.72 (d, J = 18.1 Hz, 1H), 2.61−2.68 (m, 1H), 2.32 (s, 3H), 2.12−2.29 (m, 3H), 1.66−1.92 (m, 1H); ^{13}C NMR δ 175.4, 172.8, 160.7, 152.8, 144.4, 142.4, 140.7, 137.1, 137.1, 132.4, 131.0, 130.3, 129.7, 129.6, 129.5, 129.5, 129.2, 128.7, 128.5, 128.5, 128.2, 128.0, 127.6, 125.9, 125.5, 122.1, 78.0, 67.1, 66.5, 53.7, 46.1, 34.7, 30.4, 28.1, 20.4; IR ν 1784, 1574 cm^{-1}; Anal. calcd for $C_{37}H_{30}N_4O_2$: C, 78.98; H, 5.37; N, 9.96; found: C, 79.09; H, 5.32; N, 10.01.

Spiro[2,11″]indeno-[1,2b]-quinoxaline-spiro-[3,3′]-*N*-phenylsuccinimide-4-(4-methoxyphenyl)hexahydro-1*H*-pyrrolizidine 7b. Yellow solid (251 mg, 87%); mp 184−185 °C; ^{1}H NMR δ (ppm): 6.56−8.32 (m, 17H), 4.84 (m, 1H), 4.53 (d, J = 10.2 Hz, 1H), 4.20 (d, J = 18.3 Hz, 1H), 3.83 (s, 3H), 2.95−2.97 (m, 1H), 2.70−2.80 (d and m, J = 18.3 Hz, 2H), 2.18−2.30 (m, 3H), 1.90−1.94 (m, 1H); ^{13}C NMR δ 176.2, 173.3, 159.3, 153.3, 142.9, 141.2, 131.4, 130.8, 130.2, 130.0, 129.3, 128.9, 128.7, 128.2, 127.7, 126.0, 122.6, 114.5, 78.4, 67.7, 67.0, 55.2, 53.8, 46.7, 35.2, 30.8, 28.5; IR ν 1784, 1577 cm^{-1}; Anal. calcd for $C_{37}H_{30}N_4O_3$: C, 76.80; H, 5.23; N, 9.68; found: C, 76.68; H, 5.29; N, 9.72.

Spiro[2,11″]indeno-[1,2b]-quinoxaline-spiro-[3,3′]-*N*-phenylsuccinimide-4-(4-chlorophenyl)hexahydro-1*H*-pyrrolizines 7c. Yellow solid (247 mg, 85%); mp 206−207 °C; ^{1}H NMR δ (ppm): 6.51−8.25 (m, 17H), 4.76−4.84 (m, 1H), 4.74 (d, J = 10.2 Hz, 1H), 4.03 (d, J = 18.1 Hz, 1H), 2.90−2.98 (m, 1H), 2.57−2.67 (d and m, J = 18.1 Hz, 2H), 2.10−2.25 (m, 3H), 1.82−1.87 (m, 1H); ^{13}C NMR δ 172.9, 161.0, 153.2, 144.5, 142.9, 141.2, 137.6, 134.7, 133.9, 133.2, 131.3, 131.2, 130.8, 130.5, 130.2, 130.2, 129.9, 129.4, 129.3, 129.2, 129.0, 128.9, 128.8, 128.5, 128.3, 128.2, 126.6, 126.3, 125.9, 122.6, 78.4, 76.9, 76.5, 67.9, 66.9, 53.9, 46.6, 35.4, 30.7, 28.3; IR ν1782, 1576 cm^{-1}; Anal. calcd for $C_{36}H_{27}ClN_4O_2$: C, 74.16; H, 4.67; N, 9.61; found: C, 74.06; H, 4.61; N, 9.69.

General Procedure for the Preparation of Cycloadducts 7d−h and Piperazine 8. A mixture of **3** (0.5 mmol), L-proline **2** (0.75 mmol), and acenaphthenequinone **1b** was refluxed in methanol (10 mL) for 2h. After completion of the reaction as monitored from TLC, the solvent was removed under reduced pressure, and residue was chromatographed on silica gel employing ethyl acetate-cyclohexane (3:7 v/v) as eluent to obtain the pure products **7d−h** and piperazine **8**.

Spiro[2,2″]acenaphthene-1″-one-spiro-[3,3′]-*N*-phenylsuccinimide-4-phenylhexahydro-1*H*-pyrrolizine 7d. Yellow solid (204 mg, 70%); mp 202−203 °C; ^{1}H NMR δ (ppm): 6.48−8.10 (m, 16H),

DOI: 10.1021/acs.joc.5b01399
J. Org. Chem. 2015, 80, 9064−9075

4.66 (m, 1H), 4.19 (d, J = 9.9 Hz, 1H), 3.30−3.33 (m, 1H), 3.15 (d, J = 18.4 Hz, 1H), 2.63−2.96 (m and d, J = 18.4 Hz, 2H), 1.95−2.14 (m, 2H), 1.79 (m, 1H); ^{13}C NMR δ 202.5, 177.4, 173.0, 141.7, 135.7, 134.2, 131.8, 130.9, 130.5, 130.4, 129.0, 128.6, 128.4, 127.9, 127.7, 127.5, 125.7, 125.5, 124.5, 121.8, 80.5, 67.9, 64.8, 57.5, 47.5, 34.8, 30.0, 26.6; IR ν 1787, 1715 cm^{-1}; Anal. calcd for $C_{33}H_{26}N_2O_3$: C, 79.50; H, 5.26; N, 5.62; found: C, 79.41; H, 5.33; N, 5.70.

Spiro[2,2″]acenaphthene-1″-one-spiro-[3,3′]-*N*-phenylsuccinimide-4-(4-methylphenyl)hexahydro-1*H*-pyrrolizines 7e. Yellow solid (171 mg, 67%); mp 208−209 °C; ^{1}H NMR δ (ppm): 6.54−8.61 (m, 15H), 4.68 (m, 1H), 4.21 (d, J = 10.2 Hz, 1H), 3.34−3.37 (m, 1H), 3.19 (d, J = 18.6 Hz, 1H), 2.69−2.75 (m and d, J = 18.6 Hz, 2H), 2.34 (s, 3H), 2.02−2.19 (m, 3H), 1.83−1.88 (m, 1H); ^{13}C NMR δ 205.1, 177.9, 173.6, 142.1, 137.7, 132.9, 132.3, 131.5, 131.0, 130.9, 129.8, 129.3, 129.1, 128.8, 128.4, 128.2, 126.2, 125.9, 125.1, 122.3, 80.9, 68.3, 65.3, 57.7, 48.0, 35.3, 30.4, 27.1, 21.0; IR ν 1777, 1708 cm^{-1}; Anal. calcd for $C_{34}H_{28}N_2O_3$: C, 79.67; H, 5.51; N, 5.46; found: C, 79.68; H, 5.44; N, 5.41.

Spiro[2,2″]acenaphthene-1″-one-spiro-[3,3′]-*N*-phenylsuccinimide-4-(4-methoxyphenyl)hexahydro-1*H*-pyrrolizines 7f. Yellow solid (190 mg, 75%); mp 212−212 °C; ^{1}H NMR δ (ppm): 6.45−8.10 (m, 15H), 4.58−4.61 (m, 1H), 4.13 (d, J = 9.9 Hz, 1H), 3.74 (s, 3H), 3.28−3.30 (m, 1H), 3.13 (d, J = 18.7 Hz, 1H), 2.63−2.69 (m and d, J = 18.7 Hz, 2H), 1.97−2.35 (m, 3H), 1.82−1.90 (m, 1H); ^{13}C NMR δ 202.8, 177.5, 173.1, 158.7, 131.8, 130.9, 130.5, 130.4, 130.0, 128.3, 127.9, 127.7, 127.4, 125.7, 125.4, 124.6, 121.8, 114.0, 80.4, 67.9, 64.8, 56.9, 54.7, 47.5, 34.7, 30.0, 26.6; IR ν 1776, 1710 cm^{-1}; Anal. calcd for $C_{34}H_{28}N_2O_4$: C, 77.25; H, 5.34; N, 5.30; found: C, 77.30; H, 5.28; N, 5.38.

Spiro[2,2″]acenaphthene-1″-one-spiro-[3,3′]-*N*-phenylsuccinimide-4-(4-chlorophenyl)hexahydro-1*H*-pyrrolizines 7g. Yellow solid (200 mg, 90%); mp 220−221 °C; ^{1}H NMR δ (ppm): 6.65−8.21 (m, 15H), 4.66−4.73 (m, 1H), 4.22 (d, J = 9.9 Hz, 1H), 3.41−3.50 (m, 1H), 3.15 (d, J = 18.9 Hz, 1H), 2.73−2.78 (m, 1H), 2.63 (d, J = 18.9 Hz, 1H), 2.19−2.25 (m, 2H), 1.99−2.11 (m, 1H), 1.82−1.98 (m, 1H); ^{13}C NMR δ 202.7, 178.2, 173.3, 142.3, 134.9, 134.4, 133.9, 132.4, 131.3, 130.9, 130.9, 129.5, 129.3, 129.1, 128.9, 128.5, 128.3, 128.2, 126.4, 126.1, 125.0, 122.5, 80.9, 68.8, 65.1, 57.8, 48.1, 35.5, 30.4, 26.8; IR ν 1778, 1715 cm^{-1}; Anal. calcd for $C_{33}H_{25}ClN_2O_3$: C, 74.36; H, 4.73; N, 5.26; found: C, 74.46; H, 4.81; N, 5.34.

Spiro[2,2″]acenaphthene-1″-one-spiro-[3,3′]-*N*-phenylsuccinimide-4-(4-bromophenyl)hexahydro-1*H*-pyrrolizines 7h. Yellow solid (225 mg, 78%); mp 216−217 °C;^{1}H NMR δ (ppm): 6.56−8.20 (m, 15H), 4.65−4.72 (m, 1H), 4.21 (d, J = 9.9 Hz, 1H), 3.41−3.49 (m, 1H), 3.16 (d, J = 18.7 Hz, 1H), 2.73−2.79 (m, 1H), 2.67 (d, J = 18.7 Hz, 2H), 2.18−2.25 (m, 2H), 2.00−2.07 (m, 1H), 1.85−1.88 (m, 1H); ^{13}C NMR δ 202.2, 177.7, 172.8, 141.8, 134.9, 133.9, 131.9, 131.8, 130.8, 130.4, 128.4, 128.0, 127.8, 127.7, 125.6, 124.5, 122.0, 121.6, 80.5, 68.3, 64.5, 57.3, 47.6, 35.0, 29.9, 26.3; IR ν 1712, 1778 cm^{-1}; Anal. calcd for $C_{33}H_{25}BrN_2O_3$: C, 68.64; H, 4.36; N, 4.85; found: C, 68.53; H, 4.45; N, 4.79.

General Procedure for the Preparation of Piperazines 8 and 9. A mixture of acenaphthenequinone **1b** (0.5 mmol) and L-proline **2** (0.5 mmol) was refluxed in methanol (10 mL) for 3h. After completion of the reaction, as monitored from TLC, the solvent was removed under reduced pressure, and residue was chromatographed on silica gel employing ethyl acetate-cyclohexane (1:9 v/v) as eluent to obtain the pure products **8** and **9**.

Spiro[2′,3]-bis(acenaphthene-1′-one)perhydrodipyrrolo-[1,2-a:1,2-d]-pyrazine 8. Orange solid (137 mg, 90%); mp 234−235 °C; ^{1}H NMR δ (ppm): 7.16−7.67 (m, 12H), 3.90 (m, 2H), 2.59−2.64 (m, 2H), 2.12−2.20 (m, 2H), 1.96−2.00 (m, 2H), 1.58−1.83 (m, 6H); ^{13}C NMR δ 206.4, 140.7, 136.1, 133.4, 129.9, 129.4, 127.1, 126.9, 124.0, 122.6, 118.6, 71.6, 59.8, 46.9, 27.1, 20.6; IR ν 1708, 1177 cm^{-1}; Anal. calcd for $C_{32}H_{26}N_2O_2$: C, 81.68; H, 5.57; N, 5.95; found: C, 81.60; H, 5.64; N, 5.90.

Spiro[2′,5]-bis(acenaphthene-1′-one)perhydrodipyrrolo-[1,2-a:1,2-d]-pyrazine 9. Yellow solid (74 mg, 90%); mp 244−245 °C;^{1}H NMR δ (ppm): 7.16−7.67 (m, 12H), 3.90 (m, 2H), 2.59−2.64 (m, 2H), 2.12−2.20 (m, 2H), 1.96−2.00 (m, 2H), 1.58−1.83 (m, 6H); ^{13}C NMR δ 206.4, 140.7, 136.1, 133.4, 129.9, 129.4, 127.1, 126.9, 124.0, 122.6, 118.6, 71.6, 59.8, 46.9, 27.1, 20.6; IR ν 1715, 1170 cm^{-1}; Anal. calcd for $C_{32}H_{26}N_2O_2$: C, 81.68; H, 5.57; N, 5.95; found: C, 81.73; H, 5.51; N, 6.04.

DFT Calculations. The geometric optimizations of all reactants, TS, and products were performed using the B3LYP functional and the 6-31G(d,p)[32] basis set in the Gaussian 09[33] environment, by using the Berny analytical gradient method.[34] The global electrophilicity index, ω, was calculated following the expression,[25,26] $\omega = (\mu^2/2\eta)$, where μ is the electronic chemical potential, $\mu = (E_H + E_L)/2$, and η is the chemical hardness, $\eta = (E_L - E_H)$. The Fukui condensed functions have been calculated from local populations found from single point calculations carried out on reduced, neutral, and oxidized forms with geometries optimized for neutral species. Characterizations have been performed under the same level of calculation. Vibrational analysis has been performed for all the stationary points. TS are characterized by a single negative imaginary frequency. For all TS structures, the intrinsic reaction coordinate[35] calculation, using the Hessian-based predictor−corrector method,[36] was performed to ascertain that each TS connected the expected reactants and products. Thermal corrections were computed from unscaled frequencies for a standard state of 298.15 K and 1 atm in gas phase and within the harmonic approximation.

X-ray Crystallography. Diffraction data for crystal structure determinations of **4e**, **5d**, and **7a** were collected on an Oxford Diffraction Xcalibur Sapphire 3 diffractometer at 173 K. The following softwares were used: data collection: CrysAlis CCD (Oxford Diffraction, 2006); cell refinement, data reduction andabsorption correction (multiscan): CrysAlis RED (Oxford Diffraction, 2006). Intensity data for **6d** were recorded on a Nonius Kappa Apex II diffractometer at 115 K. Softwares used for data collection and reduction: SAINT V8.27B (Bruker AXS Inc., 2012); absorption correction: multiscan (SADABS V2012/1, Bruker AXS Inc., 2012). All four structures were solved by applying direct methods (ShelXS)[37] and refined with ShelXL[37] using the Olex2 package.[38] All non-hydrogen atoms were refined anisotropically. Hydrogen atoms were refined in a riding model with isotropic temperature parameters U_{iso}(H) = parameters U_{iso}(H) set to 1.2 times U_{iso} of heavy atoms bearing them for ternary CH, secondary CH_2, aromatic CH and amide NH groups. Compound **5d** showed an ambiguous Flack parameter of 0.38(3) indicating an inversion twin, therefore it was refined using TWIN in refinement.

The crystal data, data collection and structure refinement of compounds **4e**, **5d**, **6d**, and **8** are presented in Table S3. Additional crystallographic details can be obtained free of charge from the Cambridge Crystallographic Data Centre via www.ccdc.cam.ac.uk/datarequest/cif; CCDC numbers: 1405446 for **4e**, 1405447 for **5d**, 1405448 for **6d**, and 1405449 for **8**.

■ ASSOCIATED CONTENT

Supporting Information

The Supporting Information is available free of charge on the ACS Publications website at DOI: 10.1021/acs.joc.5b01399.

Additional details on computations, including total energies and Cartesian Coordinates for computed structures and TS structures. ^{1}H NMR and ^{13}C NMR spectra for all compounds. 2D NOESY spectra for compounds **4d**, **5d** and **6d**. ORTEP plots of **4e**, **5d**, **6d** and **8** and presentations of the hydrogen bonding occurring in **4e**, **5d**, and **6d** (PDF)
(CIF)

■ AUTHOR INFORMATION

Corresponding Author

*E-mail: moheddine.askri@fsm.rnu.tn. Phone: +216 98676187.

Notes

The authors declare no competing financial interest.

DOI: 10.1021/acs.joc.5b01399
J. Org. Chem. 2015, 80, 9064−9075

■ ACKNOWLEDGMENTS

Computations have been made available thanks to the Calcul Quebec, and Compute Canada. M.K., M.M.K., and C.S. thank the CNRS and the DFG for funding.

■ REFERENCES

(1) Hartmann, T.; Witte, L. *Chemistry, Biology and Chemoecology of Pyrrolizidine Alkaloids. In Alkaloids: Chemical and Biological Perspectives*; Pelletier, Ed.; Pergamon Press: Oxford, 1995; Vol. *9*.

(2) Liddel, J. R. *Nat. Prod. Rep.* **1996**, *13*, 187−653.

(3) (a) Karthikeyan, S. V.; Bala, B. D.; Raja, V. P.; Perumal, S.; Yogeeswari, P.; Sriram, D. A. *Bioorg. Med. Chem. Lett.* **2010**, *20*, 350−353. (b) Dandia, A.; Jain, A. K.; Laxkar, A. K. *RSC Adv.* **2013**, *3*, 8422−8430.

(4) (a) Girgis, A. S. *Eur. J. Med. Chem.* **2009**, *44*, 91−100. (b) Yu, B.; Yu, D. Q.; Liu, H. M. *Eur. J. Med. Chem.* **2014**, in press, 162.

(5) Periyasami, G.; Raghunathan, R.; Surendiran, G.; Mathivanan, N. *Bioorg. Med. Chem. Lett.* **2008**, *18*, 2342−23425. Bhaskar, G.; Arun, Y.; Balachandran, C.; Saikumar, C.; Perumal, P. T. *Eur. J. Med. Chem.* **2012**, *51*, 79−91.

(6) (a) Mhaske, P. C.; Shelke, S. H.; Jadhav, R. P.; Raundal, H. N.; Patil, S. V.; Patil, A. A.; Bobade, V. D. *J. Heterocyclic Chem.* **2010**, *47*, 1415−1420. (b) Prasanna, P.; Balamurugan, K.; Perumal, S.; Yogeeswari, P.; Sriram, D. *Eur. J. Med. Chem.* **2010**, *45*, 5653−5661.

(7) (a) Raj, A. A.; Raghunathan, R.; Sridevi Kumari, M. R.; Raman, N. *Bioorg. Med. Chem.* **2003**, *11*, 407−419. (b) Thangamani, A. *Eur. J. Med. Chem.* **2010**, *45*, 6120−6126.

(8) (a) Jiang, T.; Kuhen, K. L.; Wolff, K.; Yin, H.; Bieza, K.; Caldwell, J.; Bursulaya, B.; Wu, T. Y.; He, Y. *Bioorg. Med. Chem. Lett.* **2006**, *16*, 2105−2108.

(9) García Prado, E.; García Gimenez, M. D.; De la Puerta Vázquez, R.; Espartero Sánchez, J. L.; Saenz Rodríguez, M. T. *Phytomedicine* **2007**, *14*, 280−284.

(10) (a) Cui, C.-B.; Kakeya, H.; Osada, H. *Tetrahedron* **1996**, *52*, 12651−12666. (b) Sebahar, P. R.; Williams, R. M. *J. Am. Chem. Soc.* **2000**, *122*, 5666−5667. (c) Meyers, C.; Carreira, E. M. *Angew. Chem., Int. Ed.* **2003**, *42*, 694−696.

(11) (a) Suresh Babu, A. R.; Raghunathan, R. *J. Heterocycl. Chem.* **2006**, *43*, 1357−1360. (b) Kumar, R.; Perumal, S.; Manju, S. C.; Bhatt, P.; Yogeeswari, P.; Sriram, D. *Bioorg. Med. Chem. Lett.* **2009**, *19*, 3461−3465. (c) Prasanna, P.; Balamurugan, K.; Perumal, S.; Yogeeswari, P.; Sriram, D. *Eur. J. Med. Chem.* **2010**, *45*, 5653−5661. (d) Karthikeyan, S. V.; Bala, B. D.; Raja, V. P. A.; Perumal, S.; Yogeeswari, P.; Sriram, D. *Bioorg. Med. Chem. Lett.* **2010**, *20*, 350−353. (e) Maheswari, S. U.; Balamurugan, K.; Perumal, S.; Yogeeswari, P.; Sriram, D. *Bioorg. Med. Chem. Lett.* **2010**, *20*, 7278−7282. (f) Rajesh, S. M.; Perumal, S.; Menendez, J. C.; Yogeeswari, P.; Sriram, D. *MedChemComm* **2011**, *2*, 626−630. (g) Lanka, S.; Thennarasu, S.; Perumal, P. T. *Tetrahedron Lett.* **2012**, *53*, 7052−7055. (h) Lashgari, N.; Ziarani, G. M. *ARKIVOC* **2012**, 277−320. (i) Almansour, A. I.; Ali, S.; Ali, M. A.; Ismail, R.; Choon, T. S.; Sellappan, V.; Elumalai, K. K.; Pandian, S. *Bioorg. Med. Chem. Lett.* **2012**, *22*, 7418−7421. (j) Xu, Q.; Wang, D.; Wei, Y.; Shi, M. *ChemistryOpen* **2014**, *3*, 93−98. (k) Revathy, K.; Lalitha, A. *RSC Adv.* **2014**, *4*, 279−285. (l) Lanka, S.; Thennarasu, S.; Perumal, P. T. *RSC Adv.* **2014**, *4*, 2263−2266.

(12) Fredenhagen, A.; Tamura, S. Y.; Kenny, P. T. M.; Komura, H.; Naya, Y.; Nakanishi, K.; Nishiyama, K.; Sugiura, M.; Kita, H. *J. Am. Chem. Soc.* **1987**, *109*, 4409−4411.

(13) (a) Isaka, M.; Rugseree, N.; Maithip, P.; Kongsaeree, P.; Prabpai, S.; Thebtaranonth, Y. *Tetrahedron* **2005**, *61*, 5577−5583. (b) Matviiuk, T.; Morid, G.; Lherbeta, C.; Rodriguez, F.; Pasca, M. R.; Gorichko, M.; Guidettia, B.; Voitenko, Z.; Baltasa, M. *Eur. J. Med. Chem.* **2014**, *71*, 46−52.

(14) Wróbel, M. Z.; Chodkowski, A.; Herold, F.; Gomó1ka, A.; Kleps, J.; Mazurek, A. P.; Pluciński, F.; Mazurek, A.; Nowak, G.; Siwek, A.; Stachowicz, K.; S1awinska, A.; Wolak, M. S.; Szewczyk, B.; Sata1a, G.; Bojarski, A. J.; Tur1o, J. *Eur. J. Med. Chem.* **2013**, *63*, 484−500.

(15) (a) Haddad, S.; Boudriga, S.; Akhaja, T. N.; Raval, J. P.; Porzio, F.; Soldera, A.; Askri, M.; Knorr, M.; Rousselin, Y.; Kubicki, M. M.; Rajani, D. *New J. Chem.* **2015**, *39*, 520−528. (b) Haddad, S.; Boudriga, S.; Porzio, F.; Soldera, A.; Askri, M.; Sriram, D.; Yogeeswari, P.; Knorr, M.; Rousselin, Y.; Kubicki, M. M. *RSC Adv.* **2014**, *4*, 59462−59471.

(16) (a) Boudriga, S.; Gharbi, R.; Rammah, M.; Ciamala, K. *J. Chem. Res.* **2003**, *4*, 204−207. (b) Askri, M.; Jgham, N.; Rammah, M.; Ciamala, K.; Monnier-Jobé, K.; Vebrel, J. *Heterocycles* **2007**, *71*, 289−303. (c) Wannassi, N.; Rammah, M. M.; Boudriga, S.; Rammah, M.; Jobé, K. M.; Ciamala, K.; Knorr, M.; Enescu, M.; Rousselin, Y.; Kubicki, M. M. *Heterocycles* **2010**, *81*, 2749−2762. (d) Wannassi, N.; Jelizi, H.; Rammah, M.; Ciamala, K.; Knorr, M.; Monnier-Jobé, K.; Rousselin, Y.; Kubicki, M. M.; Strohmann, C. *Heterocycles* **2012**, *85*, 835−849. (e) Jelizi, H.; Rammah, M.; Askri, M.; Rammah, M.; Ciamala, K.; Monnier-Jobe, K. *Lett. Org. Chem.* **2011**, *8*, 268−273.

(17) (a) Hazra, A.; Bharitkar, Y. P.; Chakraborty, D.; Mondal, S. K.; Singal, N.; Mondal, S.; Maity, A.; Paira, R.; Banerjee, S.; Mondal, N. B. *ACS Comb. Sci.* **2013**, *15*, 41−48. (b) Xiao, J. A.; Zhang, H. G.; Liang, S.; Ren, J. W.; Yang, H.; Chen, X. Q. *J. Org. Chem.* **2013**, *78*, 11577−11583. (c) Xu, Q.; Wang, D.; Wei, Y.; Shi, M. *ChemistryOpen* **2014**, *3*, 93−98. (d) Li, J.; Wang, J.; Xu, Z.; Zhu, S. *ACS Comb. Sci.* **2014**, *16*, 506−512. (e) Kanchithalaivan, S.; Sumesh, R. V.; Kumar, R. R. *ACS Comb. Sci.* **2014**, *16*, 566−572.

(18) (a) Pardasani, R. T.; Pardasani, P.; Chaturvedi, V.; Yadav, S. K.; Saxena, A.; Sharma, I. *Heteroat. Chem.* **2003**, *14*, 36−41. (b) Chen, G.; Yang, J.; Gao, S.; Zhang, Y.; Hao, X. *Res. Chem. Intermed.* **2015**, *41*, 4987. (c) Alimohammadi, K.; Sarrafi, Y.; Tajbakhsh, M.; Yeganegi, S.; Hamzehloueian, M. *Tetrahedron* **2011**, *67*, 1589−1597.

(19) (a) Gavaskar, D.; Suresh Babu, A. R.; Raghunathan, R.; Dharani, M.; Balasubramanian, S. *J. Organomet. Chem.* **2014**, *768*, 128−135. (b) Gavaskar, D.; Raghunathan, R.; Suresh Babu, A. R. *Tetrahedron Lett.* **2014**, *55*, 2217−2220. (c) Suresh Babu, A. R.; Gavaskar, D.; Raghunathan, R. *J. Organomet. Chem.* **2013**, *745*−*746*, 409−416. (d) Suresh Babu, A. R.; Gavaskar, D.; Raghunathan, R. *Tetrahedron Lett.* **2012**, *53*, 6676−6681.

(20) (a) Laus, G.; Brossner, D.; Senn, G.; Wurst, K. *J. Chem. Soc., Perkin Trans. 2* **1996**, 1931−1936. (b) Laus, G. *J. Chem. Soc., Perkin Trans. 2* **1998**, 315−318.

(21) (a) Zhao, Y.; Liu, L.; Sun, W.; Lu, J.; Mc Eachern, D.; Li, X.; Yu, S.; Bernard, D.; Ochsenbein, P.; Ferey, V.; Carry, J. C.; Deschamps, J. R.; Sun, D.; Wang, S. *J. Am. Chem. Soc.* **2013**, *135*, 7223−7234. (b) Aguilar, A.; Sun, W.; Liu, L.; Lu, J.; Mc Eachern, D.; Bernard, D.; Deschamps, J. R.; Wang, S. *J. Med. Chem.* **2014**, *57*, 10486−10498. (c) Sarotti, A. M.; Spanevello; Suarez, R. A.; Echeverria, G. A.; Piro, O. E. *Org. Lett.* **2012**, *14*, 2556−2559. (d) Shu, L.; Li, Z.; Gu, C.; Fishlock, D. *Org. Process Res. Dev.* **2013**, *17*, 247−256.

(22) (a) Londhe, A. V.; Gupta, B.; Kohli, S.; Pardasani, P.; Pardasani, R. T. *Z. Naturforsch., B: J. Chem. Sci.* **2006**, *61*, 213−220. (b) Pardasani, R. T.; Pardasani, P.; Jain, A.; Arora, K. *Indian J. Chem.* **2006**, *45B*, 1204−1209. (c) Arora, K.; Jose, D.; Singh, D.; Gupta, R. S.; Pardasani, P.; Pardasani, R. T. *Heteroatom Chem.* **2009**, *20*, 379−392.

(23) (a) Houk, K. N. *Acc. Chem. Res.* **1975**, *8*, 361−369. (b) Houk, K. N.; Sims, J.; Duke, R. E.; Strozier, R. W.; George, J. K. *J. Am. Chem. Soc.* **1973**, *95*, 7287−7301. (c) Houk, K. N.; Sims, J.; Watts, C. R.; Luskus, L. J. *J. Am. Chem. Soc.* **1973**, *95*, 7301−7315.

(24) Chattaraj, P. K.; Maiti, B. *J. Am. Chem. Soc.* **2003**, *125*, 2705−2710.

(25) (a) Pearson, R. G. *Hard and soft acids and bases*; Dowden, Hutchinson, and Ross: Stroudsberg, PA, 1973. (b) Pearson, R. G. *Acc. Chem. Res.* **1993**, *26*, 250−255. (c) Pearson, R. G. *Chemical hardness: Application from molecules to solid*; Wiley-VCH, Weinheim, 1997. (d) Sen, K. D. Mingos, D. M. P. *Chemical hardness: Structure and bonding*; Springer: Berlin, 1993. (e) Parr, R. G.; Yang, W. *Density functional theory of atoms and molecules*; Oxford University Press: New York, 1989. (f) Parr, P. G.; Pearson, R. G. *J. Am. Chem. Soc.* **1983**, *105*, 7512−7516. (g) Vektariene, A.; Vektaris, G.; Svoboda, J. *ARKIVOC* **2009**, *7*, 311−329.

(26) Parr, R. G.; Szentpaly, L.; Liu, S. *J. Am. Chem. Soc.* **1999**, *121*, 1922−1924.

DOI: 10.1021/acs.joc.5b01399
J. Org. Chem. 2015, 80, 9064−9075

(27) (a) Arulmozhiraja, S.; Kolandaivel, P. *Mol. Phys.* **1997**, *90*, 55−62. (b) Ayers, P. W.; Yang, W.; Bartolotti, L. J. *Chemical Reactivity Theory: A Density Functional*; Chattaraj, P. K., Ed.; CRC Press: Boca Raton, FL, 2009; chapter 18.
(28) (a) Lakshmi, N. V.; Thirumurugan, P.; Perumal, P. T. *Tetrahedron Lett.* **2010**, *51*, 1064−1068. (b) Bhella, S. S.; Pannu, A. P. S.; Elango, M.; Kapoor, A.; Hundal, M. S.; Ishar, M. P. S. *Tetrahedron* **2009**, *65*, 5928−5935. (c) Ishar, M. P. S.; Singh, G.; Kumar, K.; Singh, R. *Tetrahedron* **2000**, *56*, 7817−7828. (d) Toma, L.; Quadrelli, P.; Perrini, G.; Gandolfi, R.; Valentin, C. D.; Corsaro, A.; Caromella, P. *Tetrahedron* **2000**, *56*, 4299−4309. (e) Liu, H.; Dou, G.; Shi, D. *J. Comb. Chem.* **2010**, *12*, 292−294.
(29) (a) Chandraprakash, K.; Sankaran, M.; Uvarani, C.; Shankar, R.; Ata, A.; Dallemer, F.; Mohan, P. S. *Tetrahedron Lett.* **2013**, *54*, 3896−3901. (b) Yuvaraj, P.; Reddy, B. S. R. *Tetrahedron Lett.* **2013**, *54*, 821−827.
(30) (a) Kumar, R. S.; Rajesh, S. M.; Perumal, S.; Banerjee, D.; Yogeeswari, P.; Sriram, D. *Eur. J. Med. Chem.* **2010**, *45*, 411−422. (b) Al Mamari, K.; Ennajih, H.; Zouihri, H.; Bouhfid, R.; Ng, S. W.; Essassi, E. M. *Tetrahedron Lett.* **2012**, *53*, 2328−2331. (c) Banerjee, P.; Pandey, A. K. *RSC Adv.* **2014**, *4*, 33236−33244.
(31) Yan, L.; Yang, W.; Li, L.; Shen, Y.; Jiang, Z. *Chin. J. Chem.* **2011**, *29*, 1906−1910.
(32) (a) Becke, A. D. *J. Chem. Phys.* **1993**, *98*, 5648−5652. (b) Lee, C.; Yang, W.; Parr, R. G. *Phys. Rev. B: Condens. Matter Mater. Phys.* **1988**, *37*, 785−789.
(33) Frisch, M. J.; Trucks, G. W.; Schlegel, H. B.; Scuseria, G. E.; Robb, M. A.; Cheeseman, J. R.; Zakrzewski, V. G.; Montgomery, J. A., Jr.; Stratmann, R. E.; Burant, J. C.; Dapprich, S.; Millam, J. M.; Daniels, A. D.; Kudin, K. N.; Strain, M. C.; Farkas, O.; Tomasi, J.; Barone, V.; Cossi, M.; Cammi, R.; Mennucci, B.; Pomelli, C.; Adamo, C.; Clifford, S.; Ochterski, J.; Petersson, G. A.; Ayala, P. Y.; Cui, Q.; Morokuma, K.; Malick, D. K.; Rabuck, A. D.; Raghavachari, K.; Foresman, J. B.; Cioslowski, J.; Ortiz, J. V.; Stefanov, B. B.; Liu, G.; Liashenko, A.; Piskorz, P.; Komaromi, I.; Gomperts, R.; Martin, R. L.; Fox, D. J.; Keith, T.; Al-Laham, M. A.; Peng, C. Y.; Nanayakkara, A.; Challacombe, M. W.; Gill, P. M.; Johnson, B.; Chen, W.; Wong, M. W.; Andres, J. L., Gonzalez, C.; Head-Gordon, M.; Replogle, E. S.; Pople, J. A. *Gaussian 98*, Revision A.6; Gaussian, Inc.: Wallingford, CT , 1998.
(34) (a) Cossi, M.; Barone, V.; Cammi, R.; Tomasi, J. *Chem. Phys. Lett.* **1996**, *255*, 327−335. (b) Cances, E.; Mennucci, B.; Tomasi, J. *J. Chem. Phys.* **1997**, *107*, 3032−3041.
(35) (a) Hehre, W. J.; Radom, L.; Schleyer, P. v. R.; Pople. J. A. *Ab initio Molecular Orbital Theory*; Wiley: New York, 1986. (b) Fukui, K. *J. Phys. Chem.* **1970**, *74*, 4161−4163.
(36) (a) Hratchian, H. P.; Schlegel, H. B. *J. Chem. Theory Comput.* **2005**, *1*, 61−69. (b) Barone, V.; Cossi, M.; Tomasi, J. *J. Comput. Chem.* **1998**, *19*, 404−417.
(37) Sheldrick, G. M. *Acta Crystallogr., Sect. A: Found. Crystallogr.* **2008**, *64*, 112−122.
(38) Dolomanov, O. V.; Bourhis, L. J.; Gildea, R. J.; Howard, J. A. K.; Puschmann, H. *J. Appl. Crystallogr.* **2009**, *42*, 339−341.

DOI: 10.1021/acs.joc.5b01399
J. Org. Chem. 2015, 80, 9064−9075